รายงานวิจัยฉบับสมบูรณ์

โครงการ: แคปซูลทองหุ้มทีเซลล์ที่มีความเป็นพิษสำหรับการรักษาโรคมะเร็ง

Golden cytotoxic T cell capsule for cancer treatment

โดย ผศ. ดร.ดาครอง พิศสุวรรณ

มิถุนายน 2561

สัญญาเลขที่ RSA5880011

รายงานวิจัยฉบับสมบูรณ์

โครงการ: แคปซูลทองหุ้มทีเซลล์ที่มีความเป็นพิษสำหรับการรักษาโรคมะเร็ง

Golden cytotoxic T cell capsule for cancer treatment

ผศ. ดร. ดาครอง พิศสุวรรณ
หลักสูตรวิทยาศาสตร์และวิศวกรรมวัสดุ คณะวิทยาศาสตร์ มหาวิทยาลัยมหิดล

สนับสนุนโดยสำนักงานกองทุนสนับสนุนการวิจัย (สกว.)
และมหาวิทยาลัยมหิดล

กิตติกรรมประกาศ

โครงการนี้ได้รับการสนับสนุนเงินทุนวิจัยจากสนับสนุนโดยสำนักงานกองทุนสนับสนุนการวิจัย (สกว.) มหาวิทยาลัยมหิดล และทุนสมทบจากคณะวิทยาศาสตร์ มหาวิทยาลัยมหิดล นอกจากนี้งานวิจัยชิ้นนี้สามารถสำเร็จลุล่วงได้ดี โดยมีการสร้างความร่วมมือกับ Associate Professor Murray Killingsworth จาก University of New South Wales ประเทศออสเตรเลีย ซึ่งเป็นผู้ช่วยชาญทางด้าน electron microscope และ ดร.สุจินต์ จิระ-ชีวะนันท์ จากมหาวิทยาลัยพระจอมเกล้าธนบุรี ที่ให้คำแนะนำทางด้านวิศวกรรม และเข้ามาร่วมในโครงการนี้ จากการได้รับการสนับสนุนเงินทุนดังกล่าว ไม่เพียงแต่ส่งผลให้เกิดการสร้างองค์ความรู้ทางวิทยาศาสตร์ แต่ยังช่วยเปิดโอกาสในการผลิตนักวิจัยรุ่นใหม่ ซึ่งในโครงการนี้มีนางสาวพรธิดา วัฒนกูล นักศึกษาปริญญาโท หลักสูตรวิทยาศาสตร์และวิศวกรรมวัสดุ คณะวิทยาศาสตร์ มหาวิทยาลัยมหิดล ได้เข้ามาร่วมทำงานงานวิจัยชิ้นนี้ ขอขอบพระคุณสำนักงานกองทุนสนับสนุนการวิจัย ที่เป็นองค์กรสำคัญในการช่วยผลักดันความก้าวหน้าของวิทยาศาสตร์ของประเทศ และกรุณาสนับสนุนโครงการวิจัย

ผศ. ดร. ดาครอง พิศสุวรรณ

รายละเอียดโครงการ

สัญญาเลขที่ RSA5880011

ชื่อโครงการ (ไทย) แคปซูลทองหุ้มทีเซลล์ที่มีความเป็นพิษสำหรับการรักษาโรคมะเร็ง

ชื่อโครงการ (อังกฤษ) Golden cytotoxic T cell capsule for cancer treatment

หัวหน้าโครงการ ผศ. ดร. ดาครอง พิศสุวรรณ

สังกัดหลักสูตรวิทยาศาสตร์และวิศวกรรมวัสดุ คณะวิทยาศาสตร์ มหาวิทยาลัยมหิดล

งบประมาณ 1,500,000 บาท ระยะเวลา 3 ปี

Abstract

Encapsulation of single cells is receiving increasing attention because there is a high possibility to use this technique in various biomedical and biological applications. In the meantime, T cell-based therapy has been found to provide a high potential for cancer treatment and immunotherapeutic treatments. However, it was reported that T cells could interact with cells in the immune system of recipient during cell transplantation resulting in an occurrence of some negative effects. Due to this reason, T cells are one type of cells that are attractive to be combined with cell encapsulation technique for therapeutic purpose to avoid the problem of negative effect induction from their interaction with immune cells. Here, the demonstration of a new approach by using polystyrene sulfonate coated-gold nanorods (PSS-GNRs) to be an outer layer on the T cell surface. Jurkat T cells were used as a model cell in this study. Jurkat T cells were encapsulated with poly(allyamine hydrochloride) (PAH) and/or PSS-GNRs or polystyrene sulfonate (PSS). The investigation of biological activities of T cells encapsulated with polyelectrolytes and gold nanorods was performed. The results showed that T cells encapsulated with PSS-GNRs, PAH and PSS, or PAH alone could survive and proliferate. In the case of a co-culture system, when encapsulated Jurkat T cells were co-cultured with THP-1 macrophages, the co-cultures exhibited TNF-α production enhancement. However, the TNF-α production enhancement was not found when THP-1 macrophages were co-cultured with PSS-GNR/PAH@Jurkat or PSS/PAH@Jurkat. This indicates that the encapsulating layer could help avoid the interaction between THP-1 macrophages and Jurkat T cells that related to TNF-α induction. As well, no significant inductions of IL-2, IL-1β, and IL-6 were detected in a co-culture system. The layer of PSS-GNRs at the surface of cells of cytotoxic T cells (PSS-GNRs/PAH@CT) plus laser irradiation should also provide a benefit in increasing the efficiency for cancer destruction based cell therapy. Breast cancer cells were used as a model cell in this study. The data from this study provide promising results of the possibility of using encapsulated PSS-GNR/PAH@CT for cancer destruction.

Keyword: gold nanorods, encapsulation, cancer destruction, T cells

บทคัดย่อ

การหุ้มเซลล์เดี่ยวเป็นเทคนิคที่ได้รับความนิยมค่อนข้างสูงในการนำมาประยุกต์ใช้ทางด้านชีวการแพทย์ การบำบัดรักษาโรคมะเร็งด้วยทีเซลล์ แสดงศักยภาพในการรักษาโรคมะเร็งและการบำบัดรักษาทางด้านภูมิคุ้มกัน อย่างไรก็ตามทีเซลล์สามารถทำปฏิกิกริยากับเซลล์ในระบบภูมิคุ้มกันของผู้รับทีเซลล์เข้าร่างกายส่งผลทำเกิดผลข้างเคียงเชิงลบกับผู้รับทีเซลล์เข้าร่างกาย ด้วยเหตุผลนี้จึงมีแนวคิดในการนำทีเซลล์มาหุ้มลดปัญหาการทำปฏิกิกริยาระหว่างทีเซลล์และเซลล์ในระบบภูมิคุ้มกันซึ่งกระตุ้นให้เกิดผลเสียต่อร่างกาย งานวิจัยชิ้นนี้แสดงให้เห็นถึงเทคนิคใหม่ซึ่งนำ พอลิสไตรีนซัลโฟเนต (polystyrene sulfonate; PSS) มาหุ้มอนุภาคนาโนทองรูปแท่ง (PSS-GNRs) บนผิวของทีเซลล์ Jurkat ทีเซลล์ถูกนำมาใช้เป็นทีเซลล์ต้นแบบในการศึกษา Jurkat ทีเซลล์ถูกหุ้มด้วยพอลิอัลลิลเอมีนไฮโดรคลอไรด์ (poly(allyamine hydrochloride); PAH) และ/หรือ PSS-GNRs หรือ PSS หลังจากที่ได้มีการศึกษากิจกรรมทางชีววิทยาของทีเซลล์พบว่า Jurkat ทีเซลล์ที่หุ้มด้วย PSS-GNRs, PAH และ PSS, หรือ PAH อย่างเดียวสามารถเจริญเติบโตได้ เมื่อนำ Jurkat ทีเซลล์ไปเลี้ยงร่วมกับเซลล์ในระบบภูมิคุ้มกัน (THP-1 เซลล์) THP-1 เซลล์ ถูกกระตุ้นให้ผลิต TNF-α มากขึ้น แต่เมื่อนำ THP-1 เซลล์ ไปเลี้ยงร่วมกับ Jurkat ทีเซลล์ ที่ถูกหุ้มในรูปของPSS-GNRs/PAH@Jurkat หรือ PSS/PAH@Jurkat พบว่าไม่มีการกระตุ้นให้ THP-1 เซลล์ ผลิต TNF-α ผลการทดลองตรงนี้แสดงให้เห็นว่า ชั้นที่หุ้มผิวของ Jurkat ทีเซลล์ สามารถช่วยลดการทำปฏิกิริยาระหว่าง THP-1 เซลล์ และ Jurkat ทีเซลล์ส่งผลให้ลดการกระตุ้นการหลั่ง TNF-α รวมถึงลดการหลั่งของ IL-2, IL-1β และ IL-6 เมื่อใช้เทคนิคเดียวกันไปหุ้มทีเซลล์ที่สามารถหลั่งสารพิษ (cytotoxic ทีเซลล์) ออกมาเพื่อทำลายเซลล์มะเร็ง (PSS-GNRs/PAH@CT เซลล์) ร่วมกับการฉายแสงพบว่าสามารถเพิ่มประสิทธิภาพในการทำลายเซลล์มะเร็งเต้านมที่ใช้เป็นเซลล์มะเร็งต้นแบบในการศึกษาครั้งนี้ได้ ดังนั้นผลที่ได้จากการศึกษาในครั้งนี้ได้แสดงข้อมูลของความเป็นไปได้ที่จะนำ PSS-GNRs/PAH@CT เซลล์ ไปใช้ในการทำลายเซลล์มะเร็ง

คำสำคัญ: อนุภาคนาโนทอรูปแท่ง การหุ้มเซลล์ การทำลายเซลล์มะเร็ง ทีเซลล์

1.Introduction to the research problem and its significance

Cancer is a global disease that affects all societies and ages. Noticeably in Thailand, it has been reported that cancer is one of the most common diseases that causes illness and death in the Thai elderly (1). Furthermore, it has been reported that there is a high incident rate of various types of cancer in Thailand (2). In recent years, T cells have been used for cancer therapy. The use of specific antibodies for a target antigen on the surface of cancer cells as well as for a receptor on T cells is an alternative approach for cancer treatment (3). However, there are still limitations using this approach. For example, the difficulty in generating T cells with anti-cancer reactivity. The use of gene modification to modify the immunology properties of T cells was developed (4). However, it seems that the effectiveness of using T cell for cancer treatment by this technique still also needs to be improved. Due to above reasons, various studies are continuing to improve the efficiency of using T-cells for cancer treatment.

Recently, gold nanoparticles are of interest in various pre-clinical drug and gene delivery technologies (5). The use of gold nanoparticles for photothermal therapy of cancer cells has also been reported (6, 7). Another recent technology using cell encapsulation can also be applied for treatment of various types of cancers. In this proposed project, the intention here is to develop the science and technology by using nanomaterials and cell encapsulation techniques to increase the efficiency of cytotoxic T cell for cancer destruction. The successful outcome of this proposed project will have potentially important societal significance even though it is pre-clinical and non-medical in nature. In general, it has the high potential to stimulate the development of a new paradigm for cancer treatment. The scheme of the proposed combined technique is shown in Figure 1.

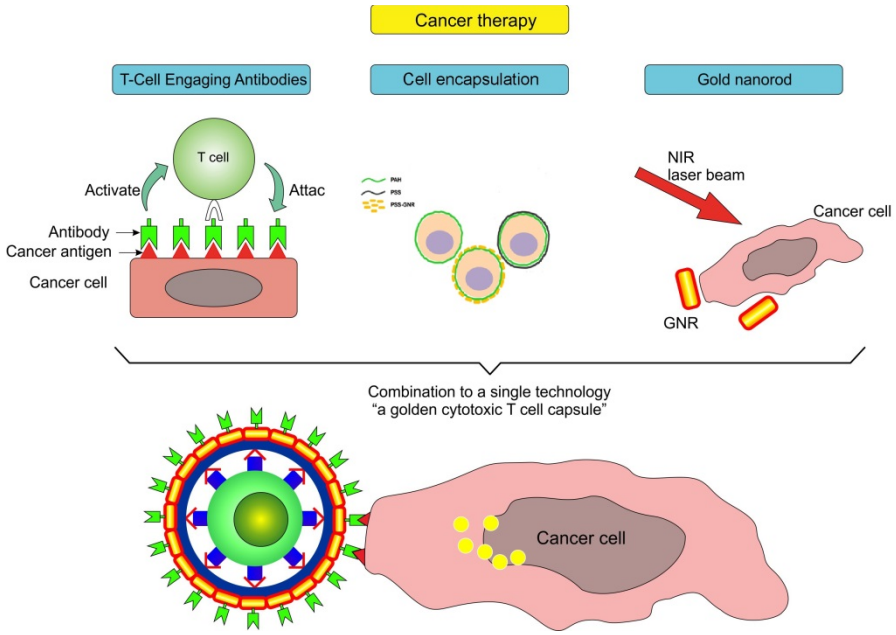

Figure 1. The scheme represents the combinations of three different approaches to a new single technology.

Objectives

This project aims to study the combination of available science technology in the field of nanotechnology and cell encapsulation to increase the efficiency of cytotoxic T cells for cancer destruction. To achieve this goal, the specific aims of this project are:

1. Engineer encapsulated T cells and explore their biological activity

2. Investigate encapsulated T cell preservation

3. Engineer cytotoxic T cells for cancer destruction. Cytotoxic T cells will be prepared by using cell encapsulation technique. This will use the similar encapsulation approach from preliminary studies and results of No.1 &2. After engineering of encapsulated cytotoxic T cells, encapsulated cytotoxic T cells are attached with bioconjugated gold nanorods that has a specific binding to target cancer cells.

4. Explore the mechanism by which encapsulated cytotoxic T cells (golden CT capsule) interact with near infrared light (NIR) and examine the efficacy and selectivity of "golden CT capsule" for targeting and killing specific cancer cells

2.Methodology

2.1. Cell culture

There were 4 cells, which are Jurkat cells, THP-1 macrophage cells, cytotoxic T cells, and breast cancer cells (MCF-7) used in this study.

Human acute T cell leukemia cell line (Jurkat cells) that used as the model cell for cell encapsulation were purchased from American Type Culture Collection (ATCC, USA). Cells were suspended in the RPMI-1640 medium supplemented with 10% FBS and 1% penicillin-streptomycin solution.

Human acute monocytic leukaemia cell line (THP-1cells) were purchased from American Type Culture Collection (ATCC, USA). Cells were suspended in the RPMI-1640 supplemented with 10% FBS and 1% penicillin-streptomycin solution. To have macrophage form of THP-1 cells, THP-1 monocyte cells were differentiated to the THP-1 macrophages by adding 25 ng ml phorbol 12-myristate 13-acetate (PMA) in a culture medium. After adding, cells were treated for 48 h. The cells were washed with RPMI-1640 medium without FBS. In this case, the non-adherent cells were removed and the adherent cells were attached on the cell culture dish. Following this, the remaining cells were incubated again with a freshly prepared PMA (25 ng/ml) in a culture medium for 48 h. After incubation, the adherent cells were washed with RPMI-1640 medium without FBS and further incubated with RPMI-1640 medium plus 10% FBS for 48 h. These adherent cells were differentiated macrophages and they were cultured in a normal culture medium for using in further experiments.

Peripheral blood lymphocytes (PBL) purchased from from JCRB cell bank were cultured in RPMI1640 medium with 10% FBS.

MCF-7 cells purchased from Riken cell bank were cultured in Dulbecco's Modified Eagle's Medium (DMEM) plus minimum essential medium (MEM) (DMEM: MEM = 1:1) supplemented with 10% of fetal bovine serum (FBS). The media were added with 1% penicillin.

All cells were cultured and maintained at 37 ºC in a humidified atmosphere incubator containing 5% CO_2.

2.2. Cytotoxic T-cell preparation.

A cluster of differentiation 3 (CD3) antibodies was used to activate T cells for cytotoxic granule induction (cytotoxic T cells; CT cells). This induction occurs after CD3 monoclonal antibody reacts with CD3 antigen expressed on T cells (8). A 96 well plate were coated with a 50 µl of anti-CD3 antibodies (clone: HIT3a; antibodies 0.05 µg/ml). The plate was incubated at 4^{o}C overnight. After incubation, the antibody solution was removed and the plate was washed 3 times with sterile phosphate buffer saline (PBS). The suspension of T-cells ($1x10^{6}$ cells/ml) was dispersed in culture media and a 200 µl of T-cells was added into a 96-well plate coated with anti-CD3 antibodies. Next, the culture was incubated at 37^{o}C in a 5% a CO_2 incubator for 3 days. Finally, T-cells were activated and changed to cytotoxic T-cells. This change was confirmed by cytotoxic molecule detection. These cytotoxic T-cells were stored in liquid nitrogen for using in further experiments.

2.3. Gold nanorods coated with PSS preparation

Commercial GNRs (~ 40 nm in width and ~ 68 nm in length) were purchased from Nanopartz™, Loveland, USA. The preparation of PSS-GNRs was performed by slightly modifying a previously published procedure (9). First, PSS-GNRs were prepared by mixing 600 µl GNRs with 300 µl PSS (M_W = 70,000 at a concentration of 2 mg/ml dissolved in 0.5 mM NaCl; Sigma Aldrich, Louis, USA) and the mixture was shaken for 30 min on a shaker at room temperature. Following this, the mixture of PSS and GNRs was centrifuged at 9391×*g* for 10 min. Next, the pellet of PSS-GNRs was dispersed in Milli-Q water for use in further experiments. To observe the morphology of PSS-GNRs, a solution containing PSS-GNRs was dropped on a copper grid. The sample was dried and then observed under TEM.

2.4. Cell encapsulation

Cell encapsulation was done by using a layer-by-layer technique of opposite charges of polyelectrolyte polymers on the cell membrane (10). Poly(allylamine hydrochloride) (PAH) cationic polymer and poly(styrene sulfonate) (PSS) anionic polymer were used in this study. Gold nanorods coated with PSS (PSS-GNRs) were also applied for cell encapsulation. The PAH solution at a concentration of 0.05 mg/ml was prepared for encapsulating cells. First, the 2 mg/ml PAH solution was dissolved in 18 mM $CaCl_2$ and used as a stock solution. This stock solution was diluted to have a concentration of 0.05 mg/ml in RPMI-1640

medium. The stock solution of 2 mg/ml PSS was prepared in RPMI-1640 medium without FBS. The PSS solution at a concentration of 0.1 mg/ml was prepared by diluting the PSS stock solution in RPMI-1640 medium without FBS. The solution of PSS-GNRs was prepared by mixing GNRs with 2 mg/ml PSS (dissolved in 0.5 mM NaCl) and shaking for 30 min at room temperature. After shaking, the solution of PSS-GNRs was washed twice with Milli-Q-water. The pellet was further used for cell encapsulation.

To encapsulate Jurkat T-cells with PAH, PAH/PSS, and PAH/PSS-GNR, Jurkat T-cells at an amount of $1x10^6$ cells were dispersed in 1 ml of RPMI-1640 supplemented with 10% FBS and 1% penicillin-streptomycin solution. Cells were centrifuged at 6,500 rpm for 5 min. After centrifugation, cells were washed with a 1 ml of RPMI-1640 without FBS and were centrifuged again. Cells were added with a 500 µl of PAH solution at a concentration of 0.05 mg/ml and were shaken for 5 min at room temperature. After this, cells were centrifuged at 6,500 rpm for 5 min and were washed with 1 ml of RPMI-1640 without FBS. This process, cells were encapsulated with PAH called here as PAH@Jurkat cells. To prepare a second layer on the surface of Jurkat T cells, a 500 µl of 0.1 mg/ml PSS solution was added to PAH@Jurkat cells. Then, cells were shaken for 10 min at room temperature. After shaking, cells were centrifuged at 6,500 rpm for 5 min and then were washed with 1 ml of RPMI-1640 without FBS. Finally, the cell encapsulation with 2 layers was obtained. This cell was called PSS/PAH@Jurkat cells. To prepare Jurkat cells that have PSS-GNR as an outer layer on the cell surface, PAH@Jurkat cells were added with a 150 µl of RPMI-1640 without FBS. Then a 50 µl of PSS-GNRs ($OD_{604\ nm}$ ~ 0.6) was added to the cells. Following this, cells were shaken for 15 min at room temperature. Next, cells were centrifuged and were washed by following the previous protocol. With this last process, encapsulated cells were called as GNR-PSS/PAH@Jurkat cells. All encapsulated cells were suspended in a culture medium supplemented with 10% FBS and 1% penicillin-streptomycin solution for use in further experiments.

2.5. Characterization of Jurkat cell encapsulation

2.5.1 Zeta potential (ζ) measurement

Encapsulated cells (PAH@Jurkat cells, PSS@Jurkat cells, PSS/PAH@Jurkat cells, and GNR-PSS/PAH@Jurkat cells) at a concentration of 1×10^6 cells/ml were dispersed in FBS-free RPMI-1640 medium. Zeta potential values of encapsulated and unencapsulated Jurkat cells and GNRs-PSS were determined by DLS (Malvern, Worcester, UK).

2.5.2 Transmission electron microscope (TEM)

A cross-section for preparation of a thin cell sample was prepared. TEM was used to observe GNR-PSS absorbed on the cell surface of GNR-PSS/PAH@Jurkat cells. The $1x10^6$ cells of non-encapsulated and GNR-PSS/PAH@Jurkat cells at a volume of 1 ml were washed once with 0.1 M sodium cacodylate buffer (SCB). The cells were fixed with 2.5% glutaraldehyde in 0.1 M of SCB at 4^oC overnight. The fixed cells were washed 3 times with 0.1 M SCB. The length of each washing was 15 min at 4^oC. Next, cells were fixed with 1% osmium tetraoxide (OsO_4) in 0.2 M of SCB at 4^oC for 1 h. Then, cells were washed 3 times gain with the same process mentioned previously. After the fixation was completed, the dehydration was performed. The encapsulated cells were dehydrated with 30%, 50%, 70%, 80%, 90%, and 95% of ethanol, for 15 min at 4^oC. Then, 100% of ethanol was added to encapsulate cells at 4^oC for 15 min. This process was done 4 times. Following this, the embedding process was prepared. The propylene oxide was mixed with 100% ethanol at a ratio of 1:1. The mixture solution was added to cells for 15 min at room temperature. The pure propylene oxide was added to cells for 15 min at room temperature. Then, the mixture of propylene oxide and araldite resin was prepared. The cells were added to a mixture solution of propylene oxide and araldite resin, at a ratio 3:1 and then incubated at room temperature for 1h. The cells were added to a mixture of propylene oxide and araldite resin (1:1) and were incubated at 4^oC for 2 days. The cells were added to a mixture of propylene oxide and araldite resin (1:3) and were incubated at room temperature overnight. Finally, the resin was polymerized in a hot air oven at 45^oC and 60^oC respectively for 2 days each. The cell samples were sent to be cut and were observed by a research collaborator in Australia, Associate Prof. Murray Killingsworth, for observation of GNRs coated with PSS on the cell surface.

2.5.3 Scanning electron microscope (SEM)

Encapsulated and unencapsulated cells were pre-fixed with 2.5% glutaraldehyde overnight. Following this, cells were fixed with 1% OsO_4 for 1 h for post-fixation. Next, cells were consequently dehydrated by soaking in 50, 60, 70, 80, 90, and 100% ethanol for 15 min (11). The critical point drying (CPD) approach was used to dehydrate biological tissues before examination by SEM. This CPD technique can help avoid damaging the surface structure of cell samples. First, cell samples were dehydrated in ethanol. After dehydration, cell samples were then placed into a CPD chamber. Then, the chamber was sealed and cooled

down to −10 °C. Next, the temperature was adjusted to 40 °C and the pressure was slowly increased to 80–120 kgf/cm^2. This condition is a CO_2 critical point. It is important to carefully monitor the temperature and the pressure to avoid sample damage. The samples were removed from the chamber when the pressure dropped to 0 kgf/cm^2. Finally, the cell samples were observed under SEM (12).

2.5.4 Fluorescence observation

Fluorescein isothiocyanate (FITC) and tetramethylrhodamine isothiocyanate (TRITC) dyes (Sigma Aldrich, Louis, USA) were conjugated with PAH by following the protocol published by (13). The conjugation of PAH to FITC (FITC-PAH) or TRITC (TRITC-PAH) was prepared by dissolving 2 mg FITC or TRITC dye in 250 µl dimethylsulphoxide (DMSO). The PAH solution was prepared by dissolving 250 mg PAH in 3 ml Milli-Q water. The pH of the PAH solution was adjusted to 8.0–8.5 using 1 M NaOH. The conjugation of PAH to FITC or TRITC dye was performed by mixing the prepared FITC or TRITC solution (250 µl) with 3 ml PAH solution (13). The mixture was then incubated overnight at room temperature in the dark. After incubation, the mixture was dialyzed to remove free dye molecules. Finally, the conjugated PAH to dye molecules was lyophilized by a freeze dryer. Standards of PAH solution at different concentrations were prepared to measure the optical density at 212 nm. This standard was used to calculate the amount of PAH in PAH-dye conjugates.

To confirm the encapsulation of Jurkat T cells into a PAH layer (PAH@Jurkat), unencapsulated Jurkat T cells (1×10^6) cells were added into a cell culture dish coated with 0.01% poly-L-lysine (PLL). Cells were then incubated in a cell incubator for 1 h and washed once with FBS-free RPMI 1640 medium. After washing, 500 µl FITC-PAH conjugates (containing 0.05 mg/ml PAH) were added into a dish and incubated in the dark for 5 min at 37 °C. Thereafter, the solution of FITC-PAH conjugates was removed. Next, the cells attached to the dish were washed twice with FBS-free RPMI-1640. In the cell fixation process, the cells attached onto the dish were fixed with 3% paraformaldehyde in PBS for 15 min at 4 °C and washed 2 times with cold PBS. Then, cold PBS was added. A green fluorescent signal was observed under the fluorescence microscope. To confirm whether the double layers of polyelectrolytes formed on the surface of encapsulated Jurkat cells (PSS/PAH@Jurkat cells), the preparation of Jurkat cells was prepared as mentioned above. For the process of encapsulation, cells were first encapsulated with 0.05 mg/ml PAH and then washed. After this, cells were encapsulated with 0.1 mg/ml PSS for 10 min at 37 °C. Thereafter, the

PSS/PAH@Jurkat cells were washed and stained with 500 µL TRITC-PAH conjugates (containing 0.05 mg/ml PAH) under dark conditions for 5 min at 37 °C. Then, cells were washed and observed under a fluorescent microscope. All washing and encapsulating processes were performed using the same approach mentioned earlier. The confirmation of GNR-PSS/PAH@Jurkat cell preparation was performed using a similar process to that described for PSS/PAH@Jurkat cells. Cells stained with fluorescent dyes (~ 5 µg/ml for 5 min) alone were also prepared as a control sample.

2.5.5 Inductively Coupled Plasma Mass Spectroscopy (ICP-MS)

In this section, ICP-MS was used to evaluate the amount of gold element that was absorbed on the cell surface. First, the $1x10^6$ cells of PSS-GNR/PAH@Jurkat and PSS-GNR@Jurkat at a volume of 1 ml were prepared in a culture medium. Then, cells were centrifuged at 5,000 rpm for 5 min. The supernatant was removed and the pellet of cells was lysed by adding 250 µl of lysis buffer (10% tween). The lysis cells were sonicated for 30 min for destruction of the cell wall. The digest buffer was prepared by mixing 3 ml of 65% HCl and 1 ml of 6% H_2O_2. Then, cells were added to 4 ml of digest buffer and were incubated overnight under dark condition in a chemical fume hood. Next 3 ml of aqua regia (3:1 of HCl: HNO_3) was added to the cells and then the cells were incubated for 2 h. Finally, the cell samples were diluted to 100 ml with Milli-Q water (sample solution contained 5% of aqua regia). Gold chloride in 5% aqua regia at the concentration of 0, 0.2, 0.5, 1.0, 2.0, 5.0, 10.0, and 20.0 µg/l (ppb) was used as a standard solution. The cell samples were measured for the quantity of gold element by using ICP-MS.

2.6. Biological activity investigation

2.6.1 Cell viability assay

To immediately measure cell viability of cells after encapsulation with PAH, PAH/PSS, and PAH/PSS-GNR, encapsulated cells at a concentration of $1x10^5$ cells/well (at a volume of 100 µl)' were seeded into a 96-well culture plate. The CellTiter-Glo® reagent was added into each well (at a volume of 100 µl) and was shaken on a shaker for 10 min. The luminescent signals were measured at a wavelength of 542 nm by using a microplate reader (SpectraMax M3 microplate reader, USA). The second step was to measure the cell viability of encapsulated cells after culturing for 24 h. The encapsulated cells with PAH, PAH/PSS and PAH/PSS-GNRs, at a concentration of $1x10^5$ cells/well in a volume 100 µl, were seeded into a 96-well culture plate. Then,

encapsulated cells were cultured in a 95% humidified air incubator at 37 ºC, and 5% CO_2 for 24 h. The CellTiter-Glo® reagent was added into each well in a volume 100 µl and shaken on a shaker for 10 min. The percentage of cell viability was calculated.

2.6.2 Cell proliferation

Different encapsulated cells were seeded into a 96-well plate (at a concentration of 1×10^4 cells per well). Cells were incubated in a cell incubator for 24, 48, and 72 h, respectively. Following the incubation, a CellTiter 96 AQueous one solution cell proliferation assay (Promega, Madison, USA) (20 µl) was used to detect cell proliferation. This process was performed following the manufacturer instructions. Unencapsulated cells were also prepared as a control.

2.6.3 Cytokine assay

The enzyme-linked immunosorbent assay (ELISA) is a technique that is used to measure cytokine production. The encapsulated cells ($1x10^5$ cells/well in a volume 100 µl) were seeded into a 96-well culture plate and were incubated for 5 and 24 h in a 95% humidified air incubator at 37 ºC, and 5% CO_2. After incubation, the supernatant was collected and stored at -80 °C until analysis. Commercial ELISA kits (BioLegend, USA) were used for IL-6, TNF-α, IL-1β and IL-2 analysis by following the manufacturer's protocol. In the first step, a monoclonal antibody (capture antibodies) was pre-coated onto the 96-well ELISA plate and was incubated overnight at 4ºC. After incubation, the unbound antibody was removed by washing 4 times with washing buffer (0.05% Tween-20 in PBS). Then, blocking buffer (1% BSA in PBS) was added and incubated for 1 h while shaking at room temperature. Then, the 96-well plate was washed 5 times with washing buffer. Standard solutions and samples were added into each and incubated for 2 h while shaking at room temperature. In this step, antigen in the sample and standard would bind with the captured antibody. Then, standard solutions and samples were washed 5 times with washing buffer for removal of the unbound substances. The detection antibody was added to each well for binding with antigen of standard and samples and was incubated for 1 h while shaking at room temperature. Following this the detection antibody was washed 5 times with washing buffer for removal of excess detection antibodies. After washing, avidin-HRP was added to bind with detection antibodies and incubated for 30 min while shaking at room temperature. After the incubation, avidin-HRP was washed 5 times with washing buffer and was washed 1 time with Milli-Q water to remove the excess avidin-HRP. TMB substrate solution was added into each well and incubated

for 15-20 mins in the dark in a 5% CO_2 incubator. A blue color developed and this color was proportional to the amount of protein or antigen in the standard and samples. Finally, a stop solution (2 N H_2SO_4) was added to measure the absorbance at a wavelength of 450 nm by using a microplate reader (SpectraMax M3 microplate reader, USA).

2.7. Cellular response of macrophage cells to encapsulated cells

Encapsulated and non-encapsulated Jurkat T-cells at a concentration of $1x10^5$ cells per well in a volume 100 µl were seeded into 96-well pate and were incubated for 5 and 24 h in a 5% CO_2 incubator at 37 ºC. The supernatant of non-encapsulated and encapsulated Jurkat T-cells were collected after culturing for 5 and 24 h. The cytokine releases of IL-6, TNF-α, IL-1β, and IL-2 analysis of encapsulated Jurkat T-cells were investigated by ELISA.

Co-culturing of THP-1 macrophage and Jurkat T-cells were prepared by seeding $5x10^4$ cells of THP-1 macrophage into a 24-well plate (at a volume of 200 µl/well). Then cells were cultured at 37°C overnight in a humidified atmosphere incubator containing a 5% CO_2. Next, the $5x10^4$ cells of Jurkat T-cells encapsulated with PAH/PSS, and PAH/PSS-GNRs, and non-encapsulated Jurkat T-cells were added into a 24 well plate (at a volume of 200µl) containing THP-1 macrophage cells and then co-cultured for 24 h. The supernatant was kept for cytokine release measurement of IL-6, IL-2, TNF-α and IL-1β by using ELISA assay.

2.8. Preservation of encapsulated cells

2.8.1 Freezing of encapsulated Jurkat T-cells

GNR-PSS/PAH@Jurkat cells, PAH@Jurkat cells, GNR-PSS/PAH@Jurkat cells were frozen in a freezing medium and were stored at -80°C (-80°C preservation) and in a liquid nitrogen tank (cryopreservation) to preserve cells for one week and one month respectively.

2.8.2 Thawing of encapsulated Jurkat T-cells and cell viability measurement

Preserved non-encapsulated and encapsulated Jurkat T-cells were thawed after storage for both one week and one month. A cryotube containing frozen cells was swirled in a 37°C water bath to thaw the cells. After thawing, a 1 ml of RPMI medium supplement with 10% FBS was added into the cryotube. The new media was added and the cell suspension was centrifuged. The supernatant was removed after centrifugation and the

cell pellet was re-suspended in RPMI medium supplemented with 10% FBS. The cell viability was measured after sudden thawing and also after culturing for 24 h by using CellTiter-Glo®. With regard to measuring the cell viability of encapsulated cells after culturing for 24 h, the thawed cells were re-suspended in a 200 µl of RPMI medium supplemented with 10% FBS and were then transferred into a 96-well plate. The encapsulated cells were cultured for 24 h at 37°C and 5% CO_2 in an incubator. After 24 h, the encapsulated cells were centrifuged at 5,000 rpm for 5 min. The supernatant was removed after centrifugation and the same steps as mentioned above were performed to investigate cell viability.

2.9. Cancer destruction by encapsulated golden cytotoxic T cells (PSS-GNR/PAH@Cytotoxic)

2.9.1 Investigation of using encapsulated cells for cancer destruction

Breast cancer cells (MCF-7 cells) were cultured in Dulbecco's Modified Eagle's Medium (DMEM) plus Minimum Essential Medium (MEM) (DMEM: MEM = 1:1) supplemented with 10% of fetal bovine serum (FBS). The media were added to with 1% penicillin and streptomycin and cells were then incubated at 37°C in a 5% CO_2 incubator. Peripheral blood lymphocyte cells (PBL) were cultured in Roswell Park Memorial Institute (RPMI) 1640 medium containing 1% penicillin/streptomycin and 10% human serum.The cells were also incubated in an incubator using the same conditions used for MCF-7 cells.

The observation of cancer destruction was done by co-culture encapsulated activated PBL cells with breast cancer cells (MCF-7 cells) and exposed to laser (635 nm and 750 nm) 500 mW for 10 min. The PSS-GNRs used in this experiment have maximum absorption at 635 nm (OD ~ 1.0) and 750 nm (OD ~ 1.0). First, MCF-7 cells at concentration $1x10^3$ cells in a volume 100 µl were seeded into a 96-well plate and incubated at 37°C in CO_2 incubator overnight. After incubation, the old medium was removed. Thereafter, $4x10^4$ cells in a volume 100 µl of encapsulated activated PBL cells were added into a 96-well plate containing MCF-7 cells. The MCF-7 cells and encapsulated activated PBL were co-cultured for 5 h. Then, cells were exposed to laser at 635 nm and 750 nm (500 mW) for 10 min. After exposure to laser, cells were co-cultured for 24 h. The PBL cells were removed and centrifuged to keep the supernatant for measuring cytotoxic molecules (granzyme B and perforin). After removed PBL cells, a 96-well plate containing MCF-7 cells was washed 3 times with sterile PBS with Ca^{2+}, Mg^{2+}. A 100 µl of RPMI free human serum was added into a 96-well plate. The percent cancer destruction was measure by using CellTiter-Glo luminescent cell viability assay.

2.10. Inductively Coupled Plasma Mass Spectroscopy (ICP-MS)

ICP-MS is an analytical technique that is used to determine the element composition of a sample. The sample was ionized with inductively coupled plasma and the mass spectroscopy was used to separate and quantify those ions. This technique is precise and sensitive (14). In this section, ICP-MS was used to evaluate the amount of gold element that was absorbed on the cell surface. First, the $1x10^6$ cells of encapsulated Jurkat T-cells with PSS-GNRs and PAH/PSS-GNRs in a volume of 1 ml were prepared in a culture medium. Then, cells were centrifuged at 5,000 rpm for 5 min. The supernatant was removed and the pellet of cells was lysed by adding 250 µl of lysis buffer (10% tween). The lysis cells were sonicated for 30 min for destruction of the cell wall. The digest buffer was prepared by mixing 3 ml of 65% HCl and 1 ml of 6% H_2O_2. Then, cell samples were added to 4 ml of digest buffer and were incubated overnight under in dark condition in a chemical fume hood. 3 ml of aqua regia (3:1 of HCl: HNO_3) was added to the cells and then the cells incubated for 2 h. Finally, the cell samples were diluted to 100 ml with Milli-Q water (sample solution contained 5% of aqua regia). Gold chloride in 5% aqua regia at the concentration of 0, 0.2, 0.5, 1.0, 2.0, 5.0, 10.0, and 20.0 µg/L (ppb) was used as a standard solution. The cell samples were measured for the quantity of gold element by using ICP-MS.

2.11. Statistical Analysis

The experiment data were expressed as mean ± standard error (SE). The statistical significance was considered as a significance at 95% confidence by using one-way analysis of variance (ANOVA) following by Bonferroni's multiple comparison test of GraphPad Prism® program.

3. Results and Discussion

3.1. PSS-GNRs and polyeletrolyte characterization

The morphology and size of PSS-GNRs were characterized by TEM as shown in Figure 2. The TEM micrographs show that PSS-GNRs were in a rod shape with an average length of ~66.91± 0.33 nm and width of ~36.66± 0.24 nm.

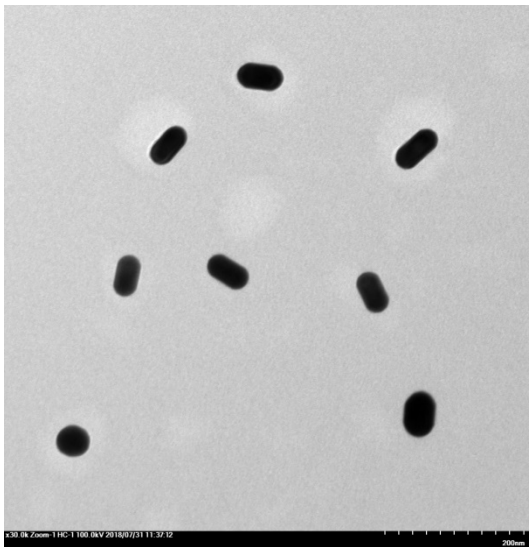

Figure 2. TEM images of PSS-GNRs.

The zeta potential of PSS-GNRs dispersed in MQ water was also determined. The result showed that the zeta potential value of PSS-GNRs was -24.8 mV. This indicates that anionic PSS molecules were coated on the surface of GNRs. The zeta potential values were measured using dynamic light scattering (DLS). Zeta potential values of 0.05 mg/ml PAH and 0.1 mg/ml PSS dispersed in RPMI-1640 medium without FBS were +11.9±0.17 mV and -27.3±1.29 mV respectively. These results were consistent with the study done by Pandey *et al.* (19). They determined the zeta potential values of PAH and PSS dispersed in 18 mM $CaCl_2$. These results showed that the zeta potential values of PAH and PSS were +32.4 mV and -20.2 mV respectively. This could indicate that PAH is a cationic polymer and PSS is an anionic polymer. However, the zeta potential values of PAH and PSS in this work had different values from Pandey *et al.*(15). This might be due to different suspension mediums or different concentration of PAH and PSS.

3.2. The confirmation of Jurkat T-cell encapsulation

3.2.1. Zeta potential of encapsulated Jurkat cells

The zeta potential values of encapsulated cells dispersed in RPMI-1640 medium without FBS were measured. The result showed that the value of zeta potential of non-encapsulated Jurkat cells (control) was -14.3±0.2 mV. This negative value could have occurred from a phosphate group of phospholipids on cell membranes. The zeta potential of encapsulated Jurkat cells PAH@Jurkat cells was -9.7±0.2 mV. This result confirmed that Jurkat cells were encapsulated with a layer of PAH, because the zeta potential value was changed and provided more positive values on the cell surface. The zeta potential of PSS@Jurkat cells was -14.6±0.4 mV and this value was similar to non-encapsulated Jurkat cells. This implies that Jurkat cells could not be encapsulated by PSS. With the two layers of encapsulation, the zeta potential of PSS/PAH@Jurkat cells was -22.2±0.2 mV. This result showed that PSS/PAH@Jurkat cells showed more negative values when compared with Jurkat cells encapsulated with PAH alone. This could be confirmed that Jurkat cells were encapsulated with PAH and then PSS. In the case of PSS-GNR/PAH@Jurkat cells, the zeta potential was around -11.3±0.4 mV and this provided more negative values than PAH@Jurkat cells. This also indicates that PSS-GNRs were absorbed on the surface of a PAH layer of Jurkat cells.

3.2.2. Fluorescent microscopy

The encapsulation on the cell surface of Jurkat cells was also investigated by using fluorescent dyes conjugated with polyelectrolytes. To confirm the encapsulation of a PAH layer, Jurkat cells were encapsulated with PAH-FITC (PAH-FITC@Jurkat). After observing under a fluorescent microscope, the distribution of green fluorescent dye was found around the cell membrane (Figure 3D). This showed that Jurkat cells were encapsulated with PAH. Pandey *et al.* (15) also used a similar technique to confirm cell encapsulation. In contrast, the control cell (cells stained with FITC-dye; FITC@Jurkat) did not show any green fluorescent signal around the cell surface (Figure 3B). The transmission mode images of Jurkat cells coated with FITC dyes and PAH-FITC@Jurkat cells are shown in Figure3A and 3C respectively.

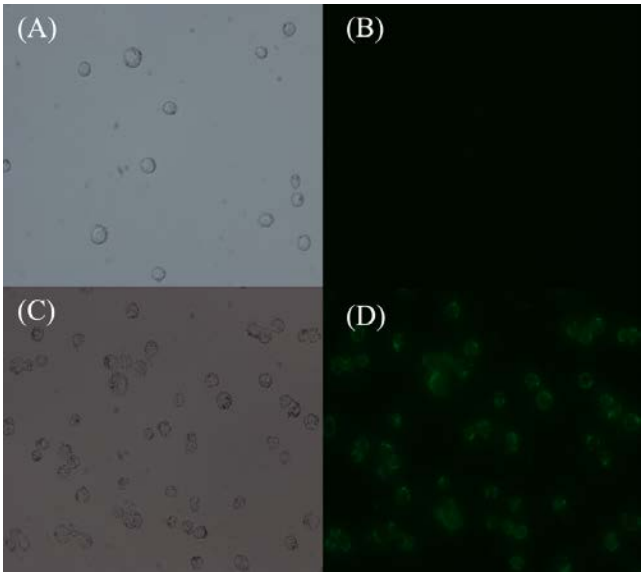

Figure 3. The microscopic image of polyelectrolyte encapsulated cells stained with PAH-FITC; Bright field of FITC@Jurkat (A) and PAH-FITC@Jurkat (C) and Fluorescent image of FITC@Jurkat (B) and PAH-FITC@Jurkat (D).

To investigate whether PSS could form a layer on cells encapsulated with PAH, the PAH polyelectrolyte was conjugated with TRITC (a red fluorescent dye). The results showed that red fluorescent signals were detected around the cell membrane of Jurkat T-cells encapsulated with PAH, PSS, and then PAH-TRITC (PAH-TRITC/PSS/PAH@Jurkat; Figure 4C, D). This implies that the second layer of PSS was formed on the cells and this second layer could bind PAH-TRITC resulting in red fluorescent signals staining around the cell surface. Similar to PAH-TRITC/PSS-GNRs/PAH@Jurkat cells, red fluorescent signals were detected around the cell surface (Figure 4E, F). But, when Jurkat cells were encapsulated with PAH and then interacted with PAH-TRITC (PAH-TRITC/PAH@Jurkat), there was no detection of fluorescent signals (Figure 4A, B).

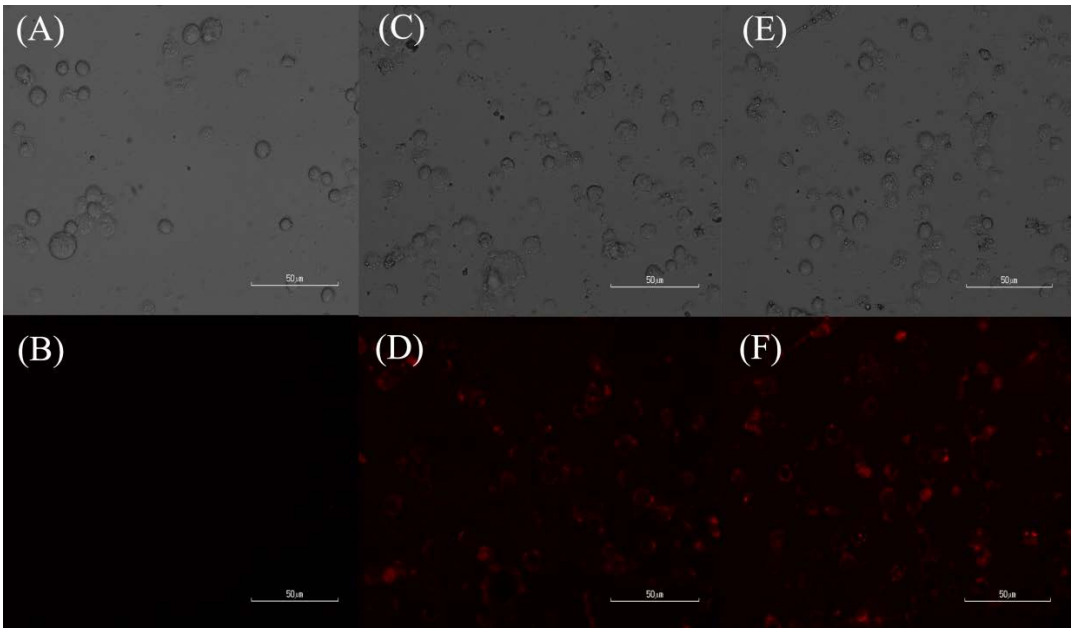

Figure 4. The microscopic image of polyelectrolyte encapsulated cells stained with PAH- TRITC; Bright and fluorescent fields of PAH-TRITC/PAH@Jurkat (A and B), PAH-TRITC/PSS/PAH@Jurkat (C and D), and PAH-TRITC/PSS-GNRs/PAH@Jurkat (E and F).

3.2.3. UV-vis spectrophotometer

GNRs have 2 dimensions from their rod shape. When GNRs are irradiated with light at a specific wavelength, the collective electrons are oscillated along the gold surface. These oscillations are localized surface plasmon resonances (LSPR). The GNRs have two distinct plasmon bands; the first band is the longitudinal plasmon band (LPB) and the second band is the transverse plasmon band (TPB) (16-18). Therefore, the combination of GNRs on the layer of encapsulated cells should be beneficial for biomedical applications. The adsorption of PSS-GNRs on the cell surface of PSS-GNRs/PAH@Jurkat Jurkat was confirmed by measuring the absorption of GNRs. The absorption of encapsulated cells was measured by using a spectrophotometer. The wavelength was scanned in ranges of 400 – 1000 nm. The result showed that the absorption peak of PSS-GNRs was at 528.5 nm and 583.5 nm respectively (Figure 5A). The absorption peak of PSS-GNRs/PAH@Jurkat has maximum peaks at wavelength 541.5 nm and 606 nm respectively (Figure 5B). This indicates that PSS-GNRs were attached on cells through the LBL technique used here.

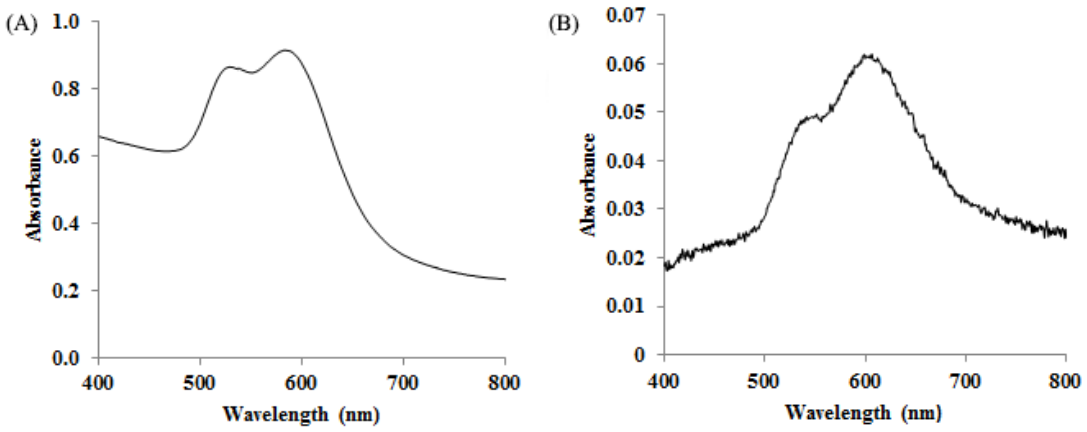

Figure 5. The light absorption spectra of PSS-GNRs (A) and of PSS-GNRs/PAH@Jurkat (B).

3.2.4. SEM and TEM

The surface morphology of cells was observed by a scanning electron microscope. As seen in Figure 6B, Encapsulated PSS-GNRs/PAH@Jurkat cells had a smooth surface that was covered with polyelectrolyte after encapsulation. A rough surface was detected in non-encapsulated cells (Figure 6A). Therefore, it can be confirmed that Jurkat cells were completely encapsulated with PAH and then PSS-GNRs.

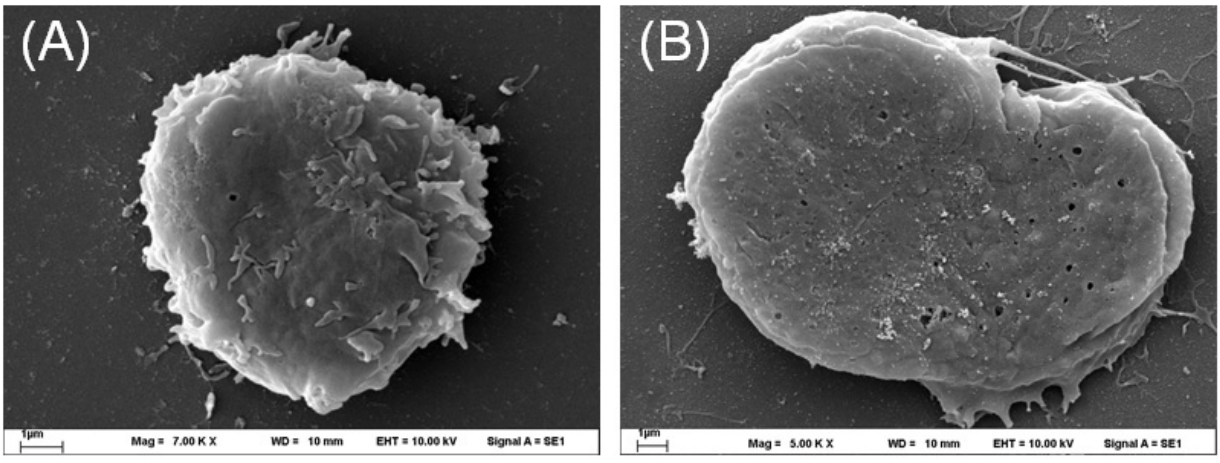

Figure 6. The SEM images of non-encapsulated Jurkat cells (Magnification = 7,000x) (A) and encapsulated PSS-GNRs/PAH@Jurkat cells(Magnification = 5,000x) (B).

Unlike SEM, the function of the TEM is based on transmitted electrons. Therefore, the sample used with TEM should be thinner than SEM. TEM technique has been used extensively to observe sections of cell samples (19). Here, the TEM technique was used to observe the localization of GNRs on the cell surface of PSS-GNRs/PAH@Jurkat cells. The TEM image shows that GNRs were located on the outer cell membrane of encapsulated cells. This confirms that Juakat T-cells were encapsulated with PAH/PSS-GNRs as shown in Figure 7.

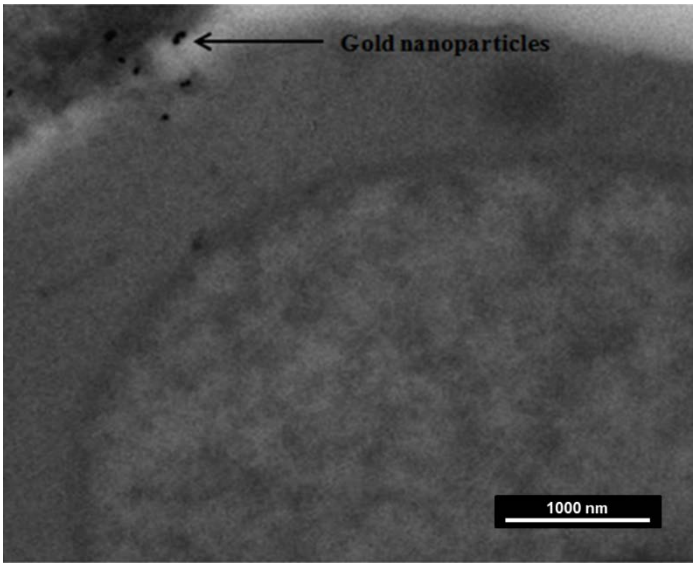

Figure 7. TEM image of a Jurkat T-cell encapsulated with PAH/PSS-GNRs.

3.2.5. ICP-MS

The quantity of gold elements attaching on the cell was determined by ICP-MS. The results showed that the encapsulated with PAH/PSS-GNRs had gold elements of around 64.30 ± 7.7 µg/l. This was significantly different from the control sample (non-encapsulated cells) (Figure 8). From these results, it can be concluded that Jurkat cells were encapsulated with PAH and PSS-GNRs. In Jurkat T-cells encapsulated with PSS-GNRs alone, a small amount of gold element (1.81 ± 0.1 µg/l) was detected.

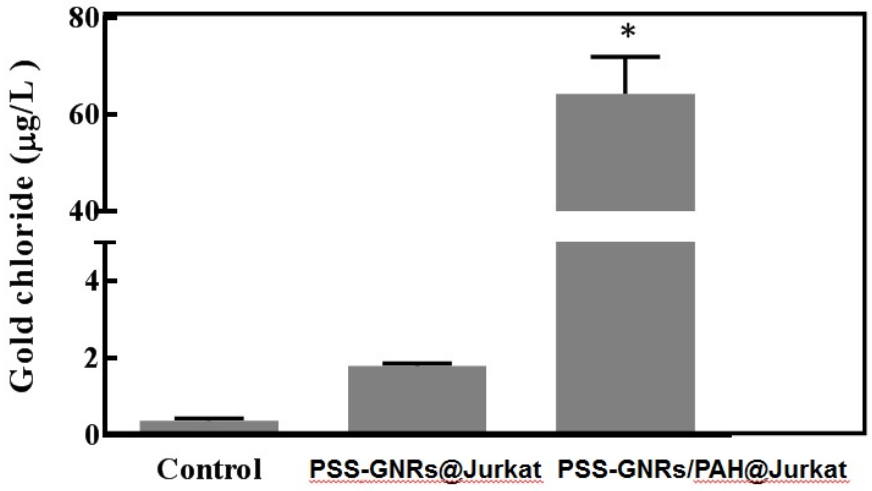

Figure 8. The amount of gold element detected from PSS-GNRs@Jurkat and PSS- GNRs/PAH@Jurkat cells. The non-encapsulated cells were used as a control. *Significantly different from non-encapsulated cells (control) ($p < 0.05$).

3.3 Cellular response of encapsulated Jurkat cells

3.3.1 Cell viability of encapsulated Jurkat cells

Encapsulated PAH@Jurkat, PSS/PAH@Jurkat, and PSS-GNRs/PAH@Jurkat cells were cultured for 0 and 24 h after encapsulation. Next, the viability of encapsulated cells was measured by using CellTiter-Glo® luminescent viability assay. The non-encapsulated cells were used as control cells. As shown in Figure 9A, PAH@Jurkat and PSS/PAH@Jurkat cells had a significant decrease in cell viability ($p<0.05$). Their cell viability was reduced to 94.44 ± 0.3% and 90.77 ± 1.24% respectively at 0 h. But, PSS-GNRs/PAH@Jurkat cells had no significant decrease in cell viability (96.73 ± 0.89%) ($p<0.05$) when compared to control cells. The viability of encapsulated Jurkat T-cells after culturing for 24 h was also investigated. The results showed that a higher effect on cell viability after 24 h as shown in Figure 9B. The cell viabilities of PAH@Jurkat, PSS/PAH@Jurkat, and PSS-GNRs/PAH@Jurkat cells after 24 h cultivation were 91.45 ± 0.6%, 85.26 ± 0.7%, and 87.04 ± 0.5% respectively. The encapsulated cells had a significant decrease in cell viability ($p<0.05$) when compared to control cells. The PAH@Jurkat cells had the highest cell viability after culturing for 24 h. The cell viability results indicate that cells after encapsulation maintained the viability more than 80%. This reflects the non-toxicity and biocompatibility of PAH or PSS polyelectrolyte or PSS-GNRs.

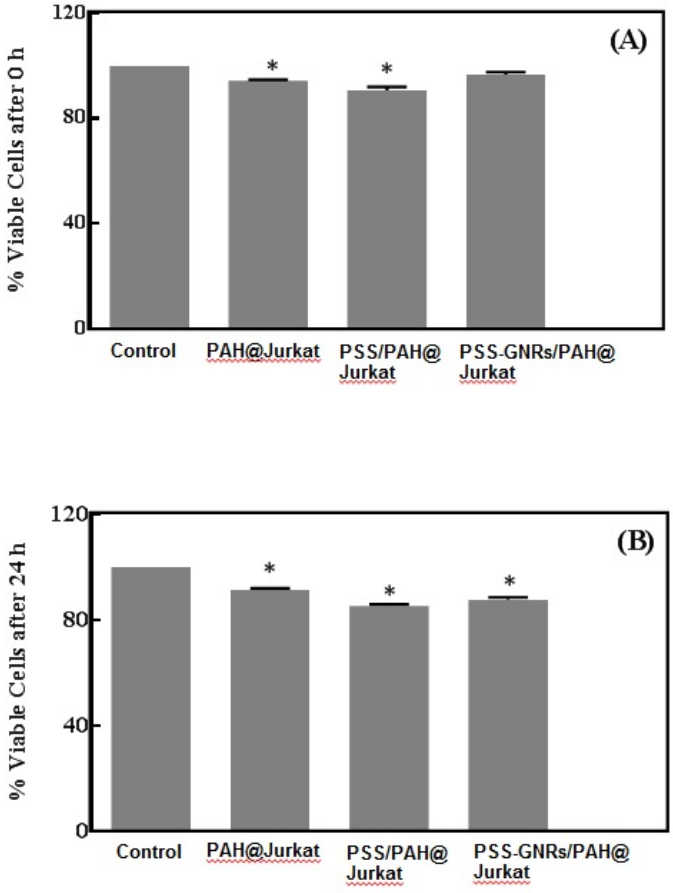

Figure 9. Cell viabilities of encapsulated PAH@Jurkat, PSS/PAH@Jurkat, and PSS-GNRs/PAH@Jurkat cells. The cell viability of cells after encapsulation for 0 h (A) and the cell viability of encapsulated Jurkat T-cells after culturing for 24 h (B). The non-encapsulated cells were used as a control. *Significantly different from non-encapsulated cells (control) ($p < 0.05$).

Many factors, such as the type of polyelectrolytes, the concentration of polyelectrolytes, and the thickness of polyelectrolyte shell, can affect cell viability of encapsulated cells. The polyelectrolyte shell should allow for nutrient diffusion and oxygen transport, which are important for cell viability (20-22). The viability of encapsulated Jurkat T-cells was reported by Pandey *et al.* (15) demonstrated that the cell viability of Jurkat T-cells encapsulated with PAH and PSS was significantly decreased but the percentage of cell viability was higher than 88% after culturing the encapsulated cells for 72 h. Similar to Diaspro *et al.*, who encapsulated single living yeast cells with PAH and PSS polyelectrolytes and reported that encapsulated yeast cells could

preserve their metabolic activities (23). Additionally, polyelectrolyte shells doped with metal nanoparticles and encapsulated to yeast cells was reported to be biocompatible and had no toxicity to yeasts (24).

3.3.2 Cell proliferation of encapsulated Jurkat cells

PAH@Jurkat, PSS/PAH@Jurkat, and PSS-GNRs/PAH@Jurkat cells were cultured for 24, 48, and 72 h respectively. The proliferation of encapsulated cells was measured by the CellTiter 96® AQ_{ueous} ONE Solution cell proliferation assay. All encapsulated Jurkat cells were able to proliferate after encapsulation and culturing for 24, 48, and 72 h respectively. The non-encapsulated cells had the highest ability to proliferate (Figure 10). Granicka *et al.* (20) encapsulated islets within threefold PLL/PEI bilayers and cultured for 8 days. They found that encapsulated cells were able to proliferate. But, the proliferation rate was two times lower than the control cell (non-encapsulated rat islets). In this work, the PSS/PAH@Jurkat, and PSS-GNRs/PAH@Jurkat at 48 and 72 h respectively, still provided good proliferation rate. Therefore, it confirmed that the encapsulated cells could maintain cell metabolic activity after encapsulation. This may be due to a low toxicity of polyelectrolytes used here resulting in less effect on cell function (15).

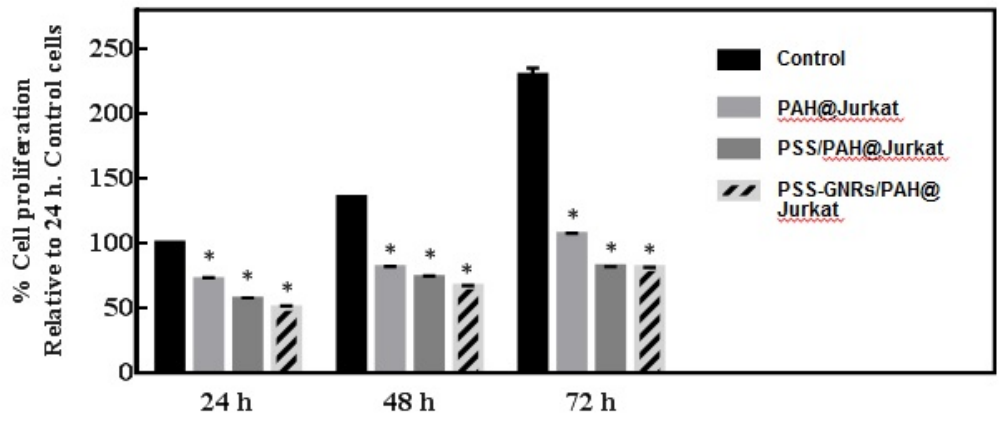

Figure 10. Cell proliferation of encapsulated PAH@Jurkat, PSS/PAH@Jurkat, and PSS-GNRs/PAH@Jurkat cells. The non-encapsulated cells were used as a control. *Significantly different from non-encapsulated cells (control) ($p < 0.05$).

3.3.3. Inflammatory cytokine release by encapsulated Jurkat cells

TNF-α, IL-6, IL-1β, and IL-2 secretion are critical parameters used for indicating the inflammatory response of T-lymphocyte cells (25). Therefore, the inflammatory responses of encapsulated PAH@Jurkat, PSS/PAH@Jurkat, and PSS-GNRs/PAH@Jurkat cells after culturing for 5 and 24 h were determined by ELISA. In Figure 11, the results showed that there were no significant inductions of TNF-α, IL-1β, and IL-2 of all encapsulated Jurkat cells cultured for 5 and 24 h ($p < 0.05$). The secretion of TNF-α of PAH@Jurkat cells (2.50 pg/ml TNF-α), PSS/PAH@Jurkat cells (2.74 pg/ml TNF-α), and PSS-GNRs/PAH@Jurkat cells (2.74 pg/ml TNF-α) at 24 h was higher than PAH@Jurkat cells (0.83 pg/ml TNF-α), PSS/PAH@Jurkat cells (0.86 pg/ml TNF-α), and PSS-GNRs/PAH@Jurkat cells (1.54 pg/ml TNF-α) at 5 h. The secretions of IL-1β from non-encapsulated cells and PAH@Jurkat, PSS/PAH@Jurkat, and PSS-GNRs/PAH@Jurkat cells at 5 h were 4.36 pg/ml, 4.26 pg/ml, 4.25 pg/ml, and 4.17 pg/ml respectively and at 24 h were 4.28 pg/ml, 4.05 pg/ml, 4.14 pg/ml, and 4.16 pg/ml respectively. In the case of IL-1β, the secretions of IL-1β of encapsulated cells at 5 and 24 h were similar to the control (non-encapsulated cell). The secretion of IL-2 at 5 h from PAH@Jurkat cells (1.52 pg/ml IL-2), PSS/PAH@Jurkat cells (2.28 pg/ml IL-2), and PSS-GNRs/PAH@Jurkat cells (1.54 pg/ml IL-2) was less than non-encapsulated cells (2.31 pg/ml IL-2). At 24 h, the secretion of IL-2 by non-encapsulated cells was 2.65 pg/ml and of cells encapsulated with PAH@Jurkat cells, PSS/PAH@Jurkat cells, and PSS-GNRs/PAH@Jurkat cells were 1.59 pg/ml, 1.92 pg/ml, and 1.31 pg/ml respectively. However, the IL-6 secretion of encapsulated cells showed a significant induction when compared with non-encapsulated cells ($p < 0.05$). The secretions of IL-6 by non-encapsulated cells at 5 and 24 h were 0.12, 0.40 pg/ml respectively. But at 5 h, PAH@Jurkat, PSS/PAH@Jurkat, and PSS-GNRs/PAH@Jurkat cells secreted IL-6 at 2.62 pg/ml, 3.56 pg/ml, and 4.24 pg/ml respectively. An increase of IL-6 levels at 24 h was also found. The IL-6 levels of PAH@Jurkat, PSS/PAH@Jurkat, and PSS-GNRs/PAH@Jurkat cells were 2.72 pg/ml, 4.94 pg/ml, and 5.11 pg/ml respectively. These results showed that the encapsulated cells at 5 and 24 h had more secretions of IL-6 than non-encapsulated cells around 20 -fold. Therefore, the encapsulated cells were induced to secrete IL-6, which is another important cytokine in acute and chronic inflammation (26).

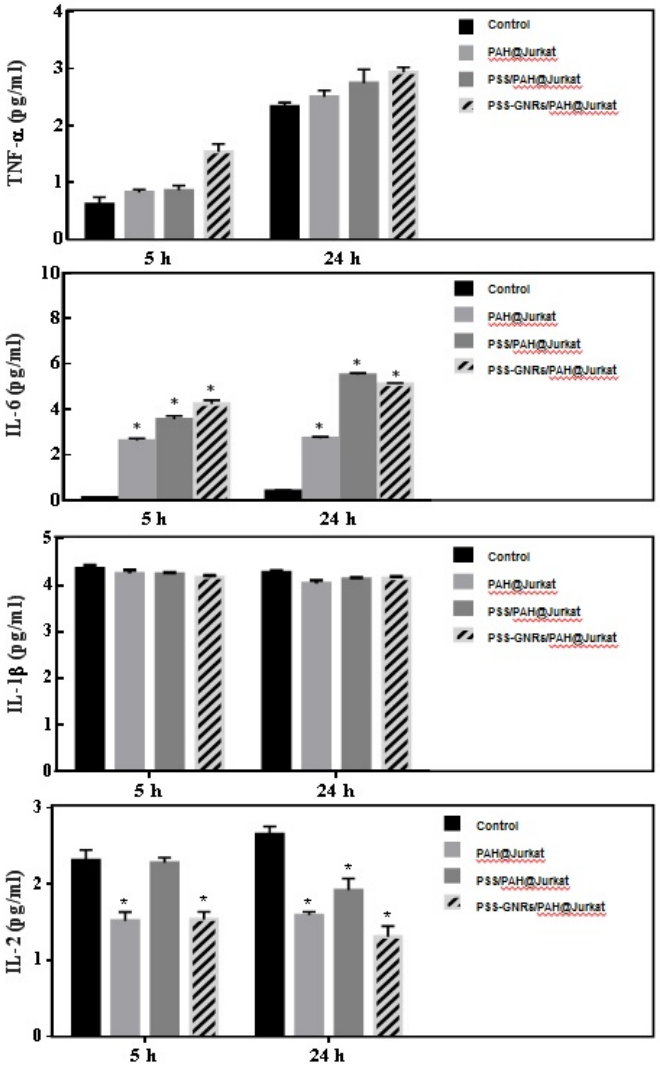

Figure 11. The cytokine production of encapsulated Juakat cells cultured for 5 and 24 h; TNF-α (A), IL-6 (B), IL-1β (C), and IL-2 (D). The inflammatory cytokine secretion was determined by ELISA. The non-encapsulated cells were used as a control. *Significantly different from control ($p < 0.05$).

Many chemicals such as concavalin A (CON A) (27) and phorbol-12-myristate-13-acetate (PMA)/phytohemagglutin (PHA) (28) can induce various cytokine productions (e.g. TNF-α , (27, 28), IL-6 (27, 28), and IL-2 (27, 28) in Jurkat cells. These chemical treatments were commonly used as a positive control group for inflammatory response induction. In this study, PMA was used as a positive control. The

Jurkat cells were treated with PMA to confirm secretion of IL-6 after encapsulation. The non-encapsulated Jurkat cells and PSS/PAH@Jurkat cells were treated with 100 ng/ml of PMA. The secretion of IL-6 was measured as shown in Figure 12. The results showed that Jurkat cells and PSS-GNRs/PAH@Jurkat cells had a significant increase of IL-6 compared with the control (non-treated Jurkat cells). The IL-6 secretion of PSS-GNRs/PAH@Jurkat cells treated with PMA was lower than non-encapsulated Jurkat cells treated with PMA. Therefore, the PSS-GNRs/PAH@Jurkat cells could induce secretion of IL-6, but at a lower level than that of non-encapsulated cells. This implies that an encapsulating layer could help protect cells from PMA.

Figure 12. The IL-6 cytokine production of non-encapsulated and encapsulated PSS-GNRs/PAH@Jurkat cells and treated with 100 ng/ml of PMA for 24 h. The inflammatory cytokine secretion was determined by ELISA. *Significantly different from control (non-treated Jurkat T-cells with PMA) ($p < 0.05$).

3.3.4. Inflammatory cytokine releases from co-culturing macrophage THP-1 cells with encapsulated Jurkat T-cells

Macrophage cells are important cells in the immune system that respond to an infection or an accumulation of damaged or dead cells. They also play an important anti-inflammatory role by releasing pro-inflammation cytokines such as TNF-α, IL-1, IL-6, IL-8, and IL-12 (29, 30). In this section, encapsulated PSS/PAH@Jurkat, PSS-GNRs/PAH@Jurkat, and non-encapsulated Jurkat T-cells were co-cultured with macrophage cells for 24 h. The cellular response in the co-culturing system was observed as to the amount of

released cytokines. The cytokine release of co-culturing cells was measured by ELISA assay. The results showed that there was no significant increase in secretions of IL-6, IL-1β, and IL-2 of co-cultured cells compared with macrophage cells cultured alone ($p<0.05$). The secretion of IL-6 from macrophage cells that were cultured alone (13.87 pg/ml IL-6) was similar to macrophage cells co-cultured with non-encapsulated cells (16.34 pg/ml IL-6), PSS/PAH@Jurkat cells (14.86 pg/ml IL-6), and PSS-GNRs/PAH@Jurkat cells (15.76 pg/ml IL-6). The secretion of TNF-α was significantly increased only when macrophage cells were co-cultured with non-encapsulated Jurkat T-cells ($p<0.05$) as shown in Figure 13. The secretions of TNF-α from macrophage cells co-cultured with PSS/PAH@Jurkat cells and PSS-GNRs/PAH@Jurkat cells were 28.18 pg/ml and 25.56 pg/ml respectively. These amounts were similar to macrophage cells cultured alone (26.81 pg/ml). The secretion of TNF-α from macrophage cells co-cultured with non-encapsulated Jurkat T-cells was 38.21 pg/ml, which was higher than TNF-α from macrophage cells cultured alone around 1.43-fold. With these results, it can be concluded that polyelectrolytes encapsulating on the cell surface could prevent an interaction between Jurkat T cells and macrophage cells. In the case of IL-1β production, the IL-1β at a concentration of 4.29 pg/ml was detected in macrophage cells co-cultured with non-encapsulated Jurkat T-cells. And, the IL-1 β at 4.31 pg/ml was found in macrophage cells co-cultured with PSS/PAH@Jurkat cells. Macrophage cells co-cultured with PSS-GNRs/PAH@Jurkat cells released IL-1β at 4.26 pg/ml. All of these amounts were closed to macrophage cells cultured alone (4.33 pg/ml). The release of IL-1β was comparable with IL-2. The IL-2 induction in macrophage cells co-cultured with non-encapsulated Jurkat cells (2.13 pg/ml) was a bit higher than ones that co-cultured with PSS/PAH@Jurkat cells (1.74 pg/ml) and PSS-GNRs/PAH@Jurkat cells (1.79 pg/ml). But, these levels were not significantly different. Thus, it could be summarized that the encapsulation of Jurkat T-cells with polyelectrolytes and polyelectrolyte-coated GNRs did not induce the macrophage cells to produce substantial inflammatory cytokines.

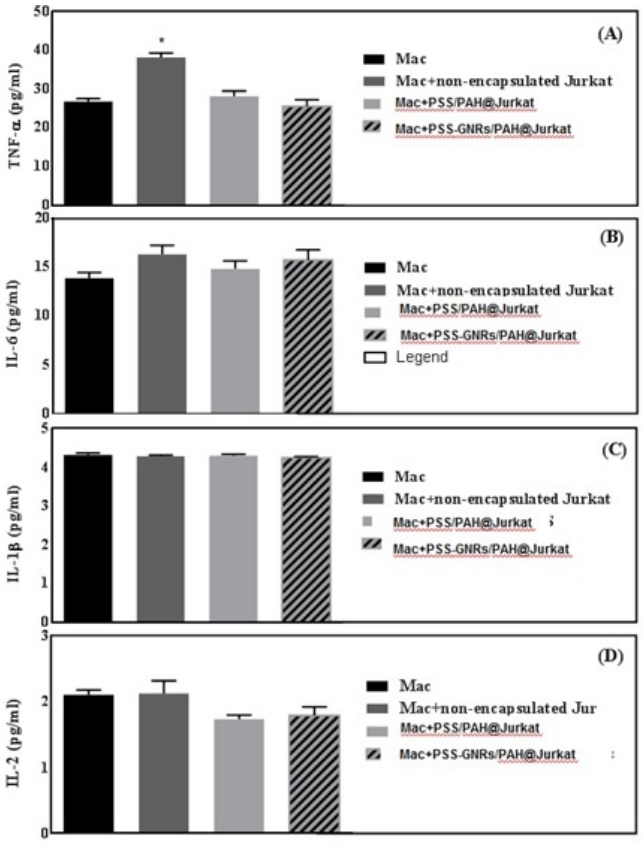

Figure 13. The cytokine production of macrophage THP-1 cells co-culture with encapsulated Juakat T-cells for 24 h; TNF-α (A), IL-6 (B), IL-1β (C), and IL-2 (D). The inflammatory cytokine secretion was determined by ELISA. *Significantly different from control (non-co culture macrophage cells) ($p < 0.05$).

3.3.5. Cell viability of co-culture macrophage THP-1 cells with encapsulated Jurkat cells

The non-encapsulated Jurkat cells and encapsulated Jurkat cells were co-cultured with macrophage THP-1 cells for 24 h. The cell viability of macrophage and Jurkat cells was measured by the Cell Titer-Glo® assay after co-culturing (Figure 14). The results showed that the cell viability of macrophage cells that co-cultured with non-encapsulated Jurkat cells (80.35 ± 0.74%), PSS/PAH@Jurkat cells (78.49 ± 0.66%) and GNRs PSS/PAH@Jurkat cells (86.52 ± 1.06%) had a significant decrease in cell viability compared with macrophage THP-1 cells cultured a lone. The Jurkat cells might secrete some substances to inhibit the growth of macrophage cells.

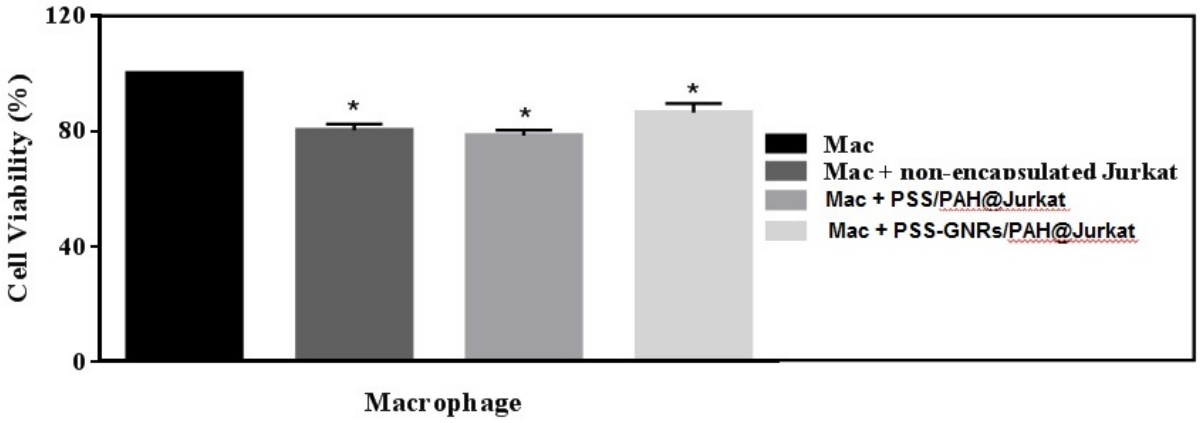

Figure 14. The cell viability of macrophage THP-1 cells and encapsulated Jurkat T-cells that co-cultured together for 24 h. The non-co-culturing cells of macrophage and Jurkat T-cells were used as a control. *Significantly different from control (non-co-culture cells) ($p < 0.05$).

3.3.6. Preservation of encapsulated cells and cell viability

To study the impact of temperature and storage environment, Jurkat cells encapsulated with PAH (PAH@Jurkat), PSS/PAH (PSS/PAH@Jurkat, and PSS-GNRs/PAH (PSS-GNRs/PAH@Jurkat) were frozen and stored in a -80^{o}C deep freezer and in a liquid nitrogen (N_2) tank for one week and one month. Cells were measured their cell viability using CellTiter-Glo® luminescent viability assay after storage. Stored cells were measured viability at 0 h (immediately after thawing) and 24 h (culturing for 24 h after thawing). The results showed that the percentages of cell viability of all encapsulated cells at 0 h and 24 h after storage at two different storage conditions mentioned previously for one week and one month were higher than 80%. It was reported that the percentage of cell viability at > 80% can be considered as non-cytotoxicity (31). Therefore, these results also indicate that our encapsulation technique could support cell viability of frozen and preserved encapsulated cells.

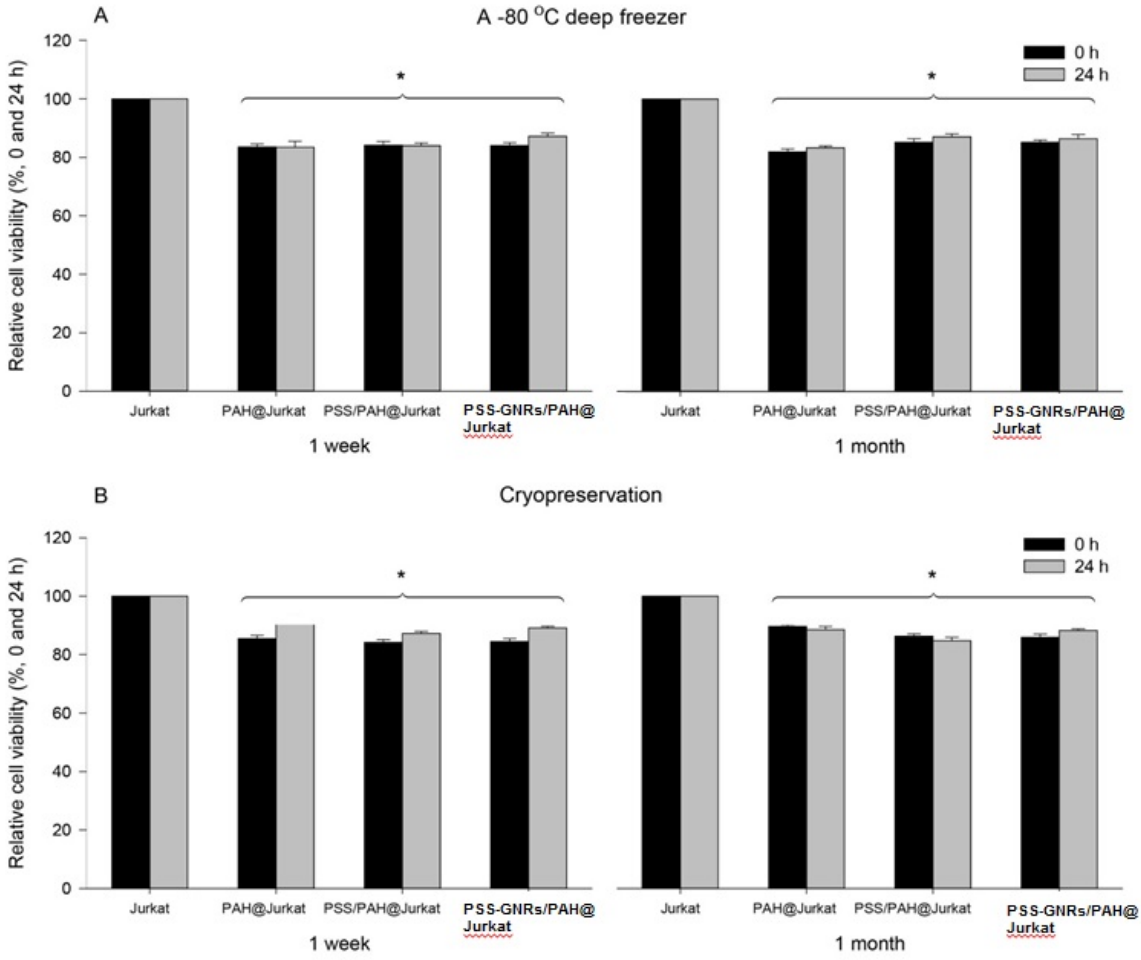

Figure 15. Cell viability of -80 °C preserved and cryopreserved encapsulated Jurkat cells for one week and one month at 0 h and 24 h (A). Non-encapsulated Jurkat cells were prepared as control cells (B). *Significant reduction of cell viability detected in different encapsulated Jurkat cells compared with non-encapsulated Jurkat cells.

3.3.7. Cancer destruction by encapsulated encapsukated cytotoxic T cells (PSS-GNRs/PAH@CT)

Besides Jurkat cells that used as the first model cells of this study, cytotoxic T-cells could also be encapsulated within layers of polyelectrolytes and GNRs. As mentioned previously, cytotoxic T-cells can destroy cancer cells. Thus, to investigate whether encapsulated cytotoxic T-cells could destroy cancer cells or not, different forms of encapsulated cytotoxic T-cells were co-cultured with MCF-7 cells for 24 h. the co-

culture with and without laser exposure was performed. The cell viabilities and the releases of toxic granules are shown in Table 1.

Table1. Cell viability of MCF- 7 cells and the releases of toxic molecules from different forms and treatment of cytotoxic T cells.

Treatment	**Cell viability (%)**	**Granzyme release (pg/ml)**	**Perforin release (pg/ml)**
MCF-7 cells	100	2.7 ± 0.54	4.71 ± 0.63
MCF-7 cells + a 635 nm laser exposure	91.92 ± 0.38	0.8 ± 0.17	4.53 ± 0.82
MCF-7 cells + a 750 nm laser exposure	90.75 ± 0.62	1.1 ± 0.36	4.46 ± 0.81
MCF-7 cells + CT	79.12 ± 0.58	405.1 ± 2.94	200.07 ± 3.64
MCF-7 cells + PSS-GNRs/PAH@CT (short GNRs)	79.97 ± 0.79	379.4 ± 6.61	178.19 ± 3.94
MCF-7 cells + PSS-GNRs/PAH@CT (short GNRs) + a 635 nm laser exposure	66.49 ± 1.02	364.1 ± 9.79	163.05 ± 2.60
MCF-7 cells + PSS-GNRs/PAH@CT (long GNRs)	75.29 ± 0.79	389.8 ± 3.56	188.54 ± 5.78
MCF-7 cells + PSS-GNRs/PAH@CT (long GNRs) + a 750 nm laser exposure	64.59 ± 0.67	345.4 ± 3.56	149.35 ± 6.03
MCF-7 cells + CT-anti HER2 antibody	66.27 ± 1.67	562.1 ± 10.66	258.25 ± 12.20
MCF-7 cells + PSS-GNRs/PAH@CT- anti HER2 antibody (short GNRs)	68.89 ± 1.77	556.3 ± 10.91	253.08 ± 19.80
MCF-7 cells + PSS-GNRs/PAH@CT- anti HER2 antibody (short GNRs) + a 635 nm laser exposure	58.75 ± 1.86	492.5 ± 5.94	191.83 ± 5.28
MCF-7 cells + PSS-GNRs/PAH@CT- anti HER2 antibody (long GNRs)	67.02 ± 1.81	531.5 ± 9.44	219.04 ± 4.84
MCF-7 cells + PSS-GNRs/PAH@CT- anti HER2 antibody (long GNRs) + a 750 nm laser exposure	55.68 ± 1.30	515.2 ± 5.50	205.37 ± 5.75

From the results shown in Table. 1, it indicates that PSS-GNRs/PAH@CT- anti HER2 antibody had the highest potential to destroy breast cancer cells. There were 2 sizes of PSS-GNRs used to encapsulate CT cells as an outer layer in this study, which were a short rod and a long rod. It showed that PSS-GNRs/PAH@CT- anti HER2 antibody (long GNRs) could kill a bit more number of breast cancer cells (% cell viability of MCF-7 = 55.68 ± 1.30%) than that of MCF-7 cells + PSS-GNRs/PAH@CT- anti HER2 antibody (short GNRs) (% cell viability of MCF-7 = 58.75 ± 1.86%) after laser irradiation. The encapsulated CT cells were able to release toxic molecules granzyme and perforin. It seems that the amount of both cytotoxic molecules from irradiated PSS-GNRs/PAH@CT- anti HER2 antibody decreased after laser irradiation. The reason for this is unclear but the reduction of these cytotoxic molecules might be loss during interaction with breast cancer cells. Overall results it showed that the encapsulated CT cells with polyelectrolytes and GNRs provide a high possibility to be used for breast cancer destruction. The death cells of MCF-7 could occur from both the heat from PSS-GNRs and the direct release of cytotoxic molecules to target MCF-7 cells.

4. Conclusions

Jurkat T-cells were successfully encapsulated with PAH/PSS or PAH/PSS-GNRs. The encapsulated cells could maintain their activities after preservation at -80 ^{o}C or cryopreservation. When applied the similar encapsulation approach to CT cells. PSS-GNRs/PAH@CT- anti HER2 antibody demonstrated a promising potential to destroy the model breast cancer cells. This study provides a new promising approach to be used for cancer destruction.

References

1. Fariha Haseen, Ramesh Adhikari, K S. Self-assessed health among Thai elderly. BMC Geriatr 2010;10(30).

2. Ahmedin Jemal, Freddie Bray, Melissa M. Center, Jacques Ferlay, Elizabeth Ward ea. Global cancer statistic. Ca Cancr J Clin 2011;61:69-90.

3. Bolhuis RH, Sturm E, E B. T cell targeting in cancer therapy. Cancer Immunol Immunother. 1991;34:1-8.

4. Michael H. Kershaw, Jennifer A. Westwood, PK D. Gene-engineered T cells for cancer therapy. Nat Rev Cancer 2013;13:525-41.

5. Pissuwan D, Niidome T, Cortie MB. The forthcoming applications of gold nanoparticles in drug and gene delivery systems. J Controll Release. 2011;149(1):65-71.

6. Pissuwan D, Valenzuela SM, Cortie MB. Therapeutic possibilities of plasmonically heated gold nanoparticles. Trends Biotechnol. 2006;24(2):62-67.

7. Pissuwan Dakrong, Valenzuela Stella, Michael CB. Prospects for gold nanorod particles in diagnostic and therapeutic applications. Biotechnol Genet Eng Rev. 2008;25:93-112.

8. JóŹwik A, Soroczyńska M, Witkowski J M, E. B. CD3 receptor modulation in Jurkat leukemic cell line. Folia Histochem Cytobiol. 2004;42:41-43.

9. Pissuwan D, Kumagai Y, NI S. Effect of surface-modified gold nanorods on the inflammatory cytokine response in macrophage cells. Part Part Syst Char. 2013;30:427–433.

10. Orive G, Maria Hernández R, Rodrıguez Gascón A, Calafiore R, Swi Chang TM, Vos Pd ea. History, challenges and perspectives of cell microencapsulation. Trends in Biotechnol.. 2004;22(2):87-92.

11. Heckman C, Kanagasundaram S, Cayer M, J P. Preparation of cultured cells for scanning electron microscope. Nat Protoc. 2007.

12. D B. Critical point drying of biological specimens for scanning electron microscopy. Supercrit Fluid Methods Protoc. 2000;13:235–243.

13. Winky LWH, Dieter WT, Nikolaus JS, Man W, Z Y. Surface-chemistry technology for microfluidics. J Micromech Microeng. 2003;13:272.

14. Kim C, Agasti SS, Zhu Z, Isaacs L, VM R. Recognition-mediated activation of therapeutic gold nanoparticles inside living cells. Nat Chem. 2010;2:962–966.

15. Pandey S, Afrin F, Tripathi RP, G G. Human T-cell line (Jurkat cell) encapsulation by nano-organized polyelectrolytes and their response assessment in vitro and in vivo. J Nanopart Res. 2013;15:1793.

16. Cao J, Sun T, KTV. G. Gold nanorod-based localized surface plasmon resonance biosensors. Sensors and Actuators B: Chemical. 2014;195:332-351.

17. Su G, Yang C, J-J. Z. Fabrication of gold nanorods with tunable longitudinal surface plasmon resonance peaks by reductive dopamine. Langmuir. 2015;31(2):817-823.

18. Takahata R, Yamazoe S, Koyasu K, T. T. Surface plasmon resonance in gold ultrathin nanorods and nanowires. J Am Chem Soc. 2014;136(24):8489-8491.

19. Winey M, Meehl JB, O'Toole ET, TH G. Conventional transmission electron microscopy. Mol Biol Cell. 2014;25(3):319-323.

20. Uludag H, De Vos P, PA. T. Technology of mammalian cell encapsulation. Adv Drug Deliv Rev. 2000;42(1-2):29-64.

21. Paredes Juárez GA, Spasojevic M, Faas MM, P. dV. Immunological and technical considerations in application of alginate-based microencapsulation systems. Front Bioeng Biotechnol. 2014;2:26.

22. N. K. The use of polymers for coating of cells. Polym Adv Technol. 2002;13(10-12):895-904.

23. Diaspro A, Silvano D, Krol S, Cavalleri O, A. G. Single living cell encapsulation in nano-organized polyelectrolyte shells. Langmuir. 2002;18(13):5047-5050.

24. Fakhrullin RF, Zamaleeva AI, Morozov MV, Tazetdinova DI, Alimova FK, Hilmutdinov AK, et al. Living fungi cells encapsulated in polyelectrolyte shells doped with metal nanoparticles. Langmuir. 2009;25(8):4628-4634.

25. Croes M, Öner FC, van Neerven D, Sabir E, Kruyt MC, Blokhuis TJ, et al. Proinflammatory T cells and IL-17 stimulate osteoblast differentiation. Bone. 2016;84:262-270.

26. Fonseca JE SM, Canhão H, Choy E. Interleukin-6 as a key player in systemic inflammation and joint destruction. Autoimmunity Rev. 2009;8(7):538-542.

27. Crowley D, O'Callaghan Y, McCarthy A, Connolly A, Piggott CO, FitzGerald RJ, et al. Immunomodulatory potential of a brewers' spent grain protein hydrolysate incorporated into low-fat milk following in vitro gastrointestinal digestion. Int J Food Sci Nutr. 2015;66(6):672-676.

28. Parnsamut C, S. B. Effects of silver nanoparticles and gold nanoparticles on IL-2, IL-6, and TNF-alpha production via MAPK pathway in leukemic cell lines. Gen Mol Res. 2015;14(2):3650-68.

29. Arango Duque G, A D. Macrophage cytokines: involvement in immunity and infectious diseases. Front Immunol. 2014;5:491.

30. CD. M. Anatomy of a discovery: M1 and M2 macrophages. Front Immunol. 2015;6:212.

31. López-García J, Lehocký M, HumpolíČek P, P. S. HaCaT keratinocytes response on antimicrobial atelocollagen substrates: Extent of cytotoxicity, cell viability and proliferation. J Funct Biomater. 2014;8(2):43-57.

Output of this research

ผลงานตีพิมพ์ในวารสารนานาชาติ

1. Wattanakull, P., Killingsworth, CM., Pissuwan, D. Biological responses of T cells encapsulated with polyelectrolyte-coated gold nanorods and their cellular activities in a co-culture system, *Applied Nanoscience*, 2017, 7(8), pp.667-679 (I.F. 2.951, Q2) *corresponding author*

บทความที่กำลังถูกพิจารณาโดยวารสารนานาชาติและบทความที่กำลังเตรียมเพื่อนำส่งให้วารสารนานาชาติพิจารณา

1. Wattanakull, P., Pissuwan, D. Characterization of T cells individually encapsulated within polyelectrolyte-coated gold nanorod shell after cryopreservation or −80 °C preservation (under consideration) *corresponding author*

2. Jiracheewanun, S., Pissuwan, D. Thermal effect of different polyelectrolyte-coated gold nanorods after irradiation, *Applied Nanoscience* (revision by following reviewers comments) *corresponding author*

3. Wattanakull, P., Pissuwan, D. Breast cancer destruction using encapsulated cytotoxic T cells combined with gold nanorods (In preparation) *corresponding author*

ผลงานตีพิมพ์ใน proceedings

1. Wattanakull, P., Pissuwan, D. Effect of encapsulated cytotoxic T-cells on cancer cell destruction, The 2nd National and International Conference on Creative Multidisciplinary Studies for Sustainable Development, The Graduate School, Silpakorn University, Bangkok, Thailand, July 20-21, 2017.

International Conference

1.Wattanakull, P., Killingsworth, CM., Pissuwan, D. Biological responses to encapsulating layers and cellular activities in a co-culture system of T cells encapsulated with PSS-coated gold nanorods, Gold 2018 Conference, UPMC, Paris, France, July 15-18, 2018.

ภาคผนวก

Appl Nanosci (2017) 7:667–679
https://doi.org/10.1007/s13204-017-0605-8

ORIGINAL ARTICLE

Biological responses of T cells encapsulated with polyelectrolyte-coated gold nanorods and their cellular activities in a co-culture system

Porntida Wattanakull[1] · Murray C. Killingsworth[2,3] · Dakrong Pissuwan[1]

Received: 1 July 2017 / Accepted: 22 September 2017 / Published online: 4 October 2017

Abstract Currently, human T cell therapy is of considerable scientific interest. In addition, cell encapsulation has become an attractive approach in biomedical applications. Here, we propose an innovative technique of single-cell encapsulation of human T cells using polyelectrolytes combined with gold nanorods. We have demonstrated encapsulation of human Jurkat T cells with poly(sodium 4-styrenesulfonate) (PSS)-coated gold nanorods (PSS-GNRs). Other forms of encapsulation, using polyelectrolytes without GNRs, were also performed. After Jurkat T cells were encapsulated with poly(allylamine hydrochloride) (PAH) and/or PSS-GNRs or PSS, most cells survived and could proliferate. Jurkat T cells encapsulated with a double layer of PSS-GNR/PAH (PSS-GNR/PAH@Jurkat) showed the highest rate of cell proliferation when compared to 24-h encapsulated cells. With the exception of IL-6, no significant induction of inflammatory cytokines (IL-2, IL-1β, and TNF-α) was observed. Interestingly, when encapsulated cells were co-cultured with THP-1 macrophages, co-cultures exhibited TNF-α production enhancement. However, the co-culture of THP-1 macrophage and PSS-GNR/PAH@Jurkat or PSS/PAH@Jurkat did not enhance TNF-α production. No significant inductions of IL-2, IL-1β, and IL-6 were detected. These data provide promising results, demonstrating the potential use of encapsulated PSS-GNR/PAH@Jurkat to provide a more inert T cell population for immunotherapy application and other biomedical applications.

Keywords Cell encapsulation · Polyelectrolytes · Gold nanorods · Biological activity · Human T cell therapy

Introduction

The transplantation of cells or tissues has been applied for treating various human diseases (Bhatia et al. 2005). Unfortunately, when using this technique, transplanted cells can be rejected by the immune system of the body. Immunosuppressant drugs are applied to solve this problem, but these drugs can cause many complications (Uludag et al. 2000). The encapsulation of cells has been developed to avoid immune rejection in cell/tissue transplantation. Furthermore, this technique can be used for other applications such as controlled delivery (Orive et al. 2014), regenerative medicine (Hunt and Grover 2010), and drug delivery (Gurruchaga et al. 2015). There are many approaches that have been used to encapsulate cells, such as, using alginate-poly cationic poly(L-lysine) (PLL) (Uludag et al. 2000), interfacial precipitation (Ai et al. 2003), and coacervation techniques (Kampf 2002). The layer-by-layer (LBL) technique is another attractive approach that can be used for cell encapsulation. This technique provides a well-defined surface, gentle conditions, nanoscale precision, and tuneable multilayer construction (Ai et al. 2003; Franz et al. 2010). Various types

Electronic supplementary material The online version of this article (doi:10.1007/s13204-017-0605-8) contains supplementary material, which is available to authorized users.

✉ Dakrong Pissuwan
dakrong.pis@mahidol.ac.th

[1] Materials Science and Engineering Program, Multidisciplinary Unit, Faculty of Science, Mahidol University, Bangkok, Thailand

[2] Electron Microscopy Laboratory, Sydney South West Pathology Service, NSW Health Pathology, Sydney, Australia

[3] Ingham Institute, Sydney, Australia

of mammalian cells, such as, human adipose mesenchymal stem cells (Granicka et al. 2014; Hachim et al. 2013), islet cells (de Vos et al. 2014), lymphocytes (Granicka et al. 2014), and human leukemia cells (Borkowska et al. 2014) have been encapsulated using this technique. The LBL encapsulation technique can also be applied for yeasts, fungi, and bacteria (Franz et al. 2010; Diaspro et al. 2002; Fakhrullin et al. 2009).

Human T lymphocytes play an important role in the immune system and have been used in immunotherapy (Juan et al. 2009; Zhao et al. 2016). Unfortunately, T lymphocytes from a donor can be activated or interact with cells in the immune system of a recipient, leading to adverse effects (Roncarolo and Battaglia 2007). Therefore, cell encapsulation of T lymphocytes might help mitigate this problem and increase the efficiency of immunotherapy in many diseases. Recently, gold nanorods (GNRs) have attracted growing interest in biological/biomedical applications. It is known that the surfaces of gold nanorods (GNRs) can be modified with polyelectrolytes through the LBL technique (Pissuwan et al. 2013; Pissuwan and Niidome 2015). This modification can reduce the toxicity of the cationic surfactant (cetyltrimethylammonium bromide; CTAB) that is commonly used to stabilize the surface of GNRs. Because of the excellent optical properties of GNRs, the combination of surface-modified GNRs, with LBL cell encapsulation, should provide substantial benefits. For example, GNRs allow for the use of a variety of characterization techniques including transmission and scanning electron microscopy, Raman spectroscopy, inductively coupled plasma mass spectrometry (ICP-MS), and spectroscopy. Furthermore, GNRs can be conjugated with various biological/chemical molecules. Therefore, rather than encapsulating cells with polymers alone, the deposition of GNRs on the surface layer of polymer-encapsulated cells can provide additional benefits. Firstly, the encapsulated cells that have GNRs fabricated on the layer of cells are able to be easily detected, or tracked, without being faced with photobleaching issues. Next, GNRs provide a high potential for a controlled release application. They can help control release of embedded therapeutic molecules after irradiating under a specific light exposure at tissue window wavelengths leading to heat energy build-up to break the capsule wall. In this work, PSS-coated gold nanorods (PSS-GNRs) were used. These types of GNRs are biocompatible and easy to conjugate with various biological molecules. Finally, the encapsulated T lymphocytes designed for therapeutic or diagnostic purposes can be used to target specific cells.

However, careful consideration is required before designing cells encapsulated with polyelectrolyte-coated gold nanorods for the applications mentioned above. It is necessary to investigate the biological responses of cells after encapsulation. Therefore, the effect of combined encapsulation with polyelectrolytes and GNRs has been assessed to clarify the impact of the coating layer on the cell surface. Furthermore, the downstream effects of this technique on other cell types such as macrophages should be assessed using a co-culture system. For these reasons, we aimed to encapsulate human Jurkat T cells using the LBL technique. These cells acted as a template for encapsulating two polyelectrolytes: poly(sodium 4-styrenesulfonate) (PSS) and poly(allylamine hydrochloride) (PAH). The final layer on the encapsulated cells consisted of GNRs coated with PSS (PSS-GNRs). A characterization of encapsulated human Jurkat T cells was performed. To our knowledge, there are only a few reports regarding the encapsulation of T lymphocytes (Pandey et al. 2013) and no reports using GNRs to encapsulate T lymphocytes. We examined the biological responses of encapsulated cells. To examine the host response to encapsulated human Jurkat T cells, a co-culture system of human macrophages and encapsulated cells was also utilized. Our proposed model of cell encapsulation and information on biological cellular responses demonstrates the possibility of applying this technique for future biomedical applications.

Materials and methods

Preparation of poly(styrene sulfonate)-coated gold nanorods

Commercial GNRs ($\sim$ 40 nm in width and $\sim$ 68 nm in length) were purchased from Nanopartz^{TM}, Loveland, USA. The preparation of PSS-GNRs was performed by slightly modifying a previously published procedure (Pissuwan et al. 2013). First, PSS-GNRs were prepared by mixing 600 µL GNRs with 300 µL PSS ($M_W = 70{,}000$ at a concentration of 2 mg mL^{-1} dissolved in 0.5 mM NaCl; Sigma Aldrich, Louis, USA) and the mixture was shaken for 30 min on a shaker at room temperature. Following this, the mixture of PSS and GNRs was centrifuged at $9391 \times g$ for 10 min. Next, the pellet of PSS-GNRs was dispersed in Milli-Q water for use in further experiments. The morphology of the GNRs was examined by transmission electron microscopy (TEM).

Cell culture

Human Jurkat T cells (ATCC) and THP-1 macrophages were cultured in Roswell Park Memorial Institute (RPMI) 1640 medium supplemented with 10% fetal bovine serum (FBS) plus 1% penicillin/streptomycin. Cells were maintained at 37 °C in a 5% CO_2 incubator.

Cell encapsulation preparation

PAH ($M_W = 15{,}000$; Sigma Aldrich, Louis, USA) was dissolved in 18 mM $CaCl_2$ to have a stock concentration of 2 mg mL^{-1}. Jurkat T cells at a concentration of 1×10^6 cells mL^{-1} (in RPMI-1640 medium without FBS) were incubated with 0.05 mg mL^{-1} PAH (diluted from the stock solution using FBS-free RPMI-1640 medium) on a shaker for 5 min at room temperature. Thereafter, the free PAH was removed by centrifugation (6500 rpm, 5 min). The cells coated with PAH were named here as PAH@-Jurkat cells. PAH@Jurkat cells were then incubated with 0.1 mg mL^{-1} PSS (dissolved in FBS-free RPMI-1640 medium) on a shaker for 10 min at room temperature. Next, the same process mentioned above was used to remove free PSS. To prepare Jurkat cells coated with PSS-GNRs (PSS-GNR/PAH@Jurkat cells), PAH@Jurkat cells were firstly prepared and then a 150 μL of FBS-free RPMI-1640 medium was added into cells. Following this step, 50 μL PSS-GNRs ($OD_{604nm} \sim 0.6$) was added into the cell mixture and incubated on a shaker for 15 min at room temperature. Next, cells were centrifuged to remove free PSS-GNRs. Finally, PAH@Jurkat and PSS-GNR/PAH@-Jurkat cells were suspended in RPMI-1640 medium plus 10% FBS for use in further experiments.

Cell encapsulation characterization

The successful encapsulation of Jurkat T cells was confirmed using various techniques.

Fluorescence observation

Fluorescein isothiocyanate (FITC) and tetramethylrhodamine isothiocyanate (TRITC) dyes (Sigma Aldrich, Louis, USA) were conjugated with PAH by following the protocol published by Winky et al. (2003). The conjugation of PAH to FITC (PAH–FITC) or TRITC (PAH–TRITC) was prepared by dissolving 2 mg FITC or TRITC dye in 250 μL dimethylsulphoxide (DMSO). The PAH solution was prepared by dissolving 250 mg PAH in 3 mL Milli-Q water. The pH of the PAH solution was adjusted to 8.0–8.5 using 1 M NaOH. The conjugation of PAH to FITC or TRITC dye was performed by mixing the prepared FITC or TRITC solution (250 μL) with 3 mL PAH solution (Winky et al. 2003). The mixture was then incubated overnight at room temperature in the dark. After incubation, the mixture was dialyzed to remove free dye molecules of FITC or TRITC by a 3.5 kDa molecular weight cut off membrane (Cellu Sep H1, Texas, USA). Finally, the conjugated PAH to dye molecules was lyophilized by a freeze dryer. Standards of PAH solution at different concentrations were prepared to measure the optical density at 212 nm. This standard was used to calculate the amount of PAH in PAH-dye conjugates.

To confirm the encapsulation of Jurkat T cells into a PAH layer (PAH@Jurkat), unencapsulated Jurkat T cells (1×10^6) cells were added into a cell culture dish coated with 0.01% poly-L-lysine (PLL). Cells were then incubated in a cell incubator for 1 h and washed once with FBS-free RPMI 1640 medium. After washing, 500 μL PAH-FITC conjugates (containing 0.05 mg mL^{-1} PAH) were added into a dish and incubated in the dark for 5 min at 37 °C. Thereafter, the solution of PAH-FITC conjugates was removed. Next, the cells attached to the dish were washed twice with FBS-free RPMI-1640. In the cell fixation process, the cells attached onto the dish were fixed with 3% paraformaldehyde in PBS for 15 min at 4 °C and washed 2 times with cold PBS. Then, cold PBS was added. A green fluorescent signal was observed under the fluorescence microscope. To confirm whether the double layers of polyelectrolytes formed on the surface of encapsulated Jurkat cells (PSS/PAH@Jurkat cells), the preparation of Jurkat cells was prepared as mentioned above. For the process of encapsulation, cells were first encapsulated with 0.05 mg mL^{-1} PAH and then washed. After this, cells were encapsulated with 0.1 mg mL^{-1} PSS for 10 min at 37 °C. Thereafter, the PSS/PAH@Jurkat cells were washed and stained with 500 μL PAH–TRITC conjugates (containing 0.05 mg mL^{-1} PAH) under dark conditions for 5 min at 37 °C. Then, cells were washed and observed under a fluorescent microscope. All washing and encapsulating processes were performed using the same approach mentioned earlier. The confirmation of PSS-GNR/PAH@Jurkat cell preparation was performed using a similar process to that described for PSS/PAH@Jurkat cells. Cells stained with fluorescent dyes ($\sim$ 5 μg mL^{-1} for 5 min) alone were also prepared as a control sample.

Transmission electron microscopy (TEM)

PSS-GNR/PAH@Jurkat cells were fixed with 2.5% glutaraldehyde (in 0.1 M sodium cacodylate buffer (SCB) pH7.4 overnight). The post-fixation was performed by fixing encapsulated and unencapsulated cells with 1.0% osmium tetroxide (OsO_4) for 4 h at room temperature. Thereafter, the cell samples were dehydrated in 30, 50, 70, 80, and 90% ethanol, respectively. This process was performed twice (15 min soaking time at each concentration of ethanol). After this, cells were soaked in 100% ethanol 4 times for 15 min each time. Following dehydration, cells were embedded in araldite resin and cell samples were cut to a thickness of 90 nm and stained with 2% uranyl acetate followed by lead citrate. The samples were then observed under TEM at 80 kV (FEI Morgagni 268D, Netherlands). Unencapsulated cells were prepared as a control. To

observe the morphology of PSS-GNRs, a solution containing PSS-GNRs was dropped on a copper grid. The sample was dried and then observed under TEM.

Scanning electron microscope (SEM)

Encapsulated and unencapsulated cells were pre-fixed with 2.5% glutaraldehyde overnight. Following this, cells were fixed with 1% OsO_4 for 1 h for post-fixation. Next, cells were consequently dehydrated by soaking in 50, 60, 70, 80, 90, and 100% ethanol for 15 min (Heckman et al. 2007). The critical point drying (CPD) approach was used to dehydrate biological tissues before examination by SEM. This CPD technique can help avoid damaging the surface structure of cell samples. First, cell samples were dehydrated in ethanol. After dehydration, cell samples were then placed into a CPD chamber. Then, the chamber was sealed and cooled down to −10 °C. Next, the temperature was adjusted to 40 °C and the pressure was slowly increased to 80–120 kgf cm^{-2}. This condition is a CO_2 critical point. It is important to carefully monitor the temperature and the pressure to avoid sample damage. The samples were removed from the chamber when the pressure dropped to 0 kgf cm^{-2}. Finally, the cell samples were observed under SEM (Bray 2000).

Zeta potential measurement

Encapsulated cells (PAH@Jurkat cells, PSS@Jurkat cells, PSS/PAH@Jurkat cells, and PSS-GNR/PAH@Jurkat cells) at a concentration of 1×10^6 cells mL^{-1} were dispersed in FBS-free RPMI-1640 medium. Zeta potential values of encapsulated and unencapsulated Jurkat T cells and PSS-GNRs were determined by DLS (Malvern, Worcester, UK).

Gold element analysis by ICP-MS

Encapsulated and unencapsulated Jurkat T cells at a concentration of 1×10^6 cells per tube were lysed using 250 μL lysis buffer [10% tween-20 dissolved in phosphate buffer saline (PBS)]. Cells were sonicated for 30 min to destroy the cell membrane. After sonication, cells were digested in a digest buffer (3 mL 65% HCl mixed with 1 mL 6% H_2O_2) with overnight incubation in the dark inside a fume hood. The aqua regia (a 3:1 ratio of HCl to HNO_3) was prepared. Thereafter, 3 mL aqua regia was added into cell samples and incubated for 2 h (Kim et al. 2010). Finally, the cell samples were adjusted to a volume of 100 mL using Milli-Q water. The final concentration of aqua regia in the sample was 5% of the total volume of the sample. A standard gold chloride solution (containing 5% aqua regia) at concentrations of 0, 0.2, 0.5, 1.0, 2.0, 5.0, 10.0, and 20.0 μg L^{-1} (ppb) was prepared.

Cell viability

Different types of encapsulated Jurkat T cells at a concentration of 1×10^5 cells per well were added into a 96-well plate. Then, encapsulated cells were cultured for 24 h in a 5% CO_2 incubator. The cell viability of encapsulated cells was directly determined using a CellTiter-Glo luminescent cell viability assay (Promega, Madison, USA). The measurement was performed following the manufacturer's instructions. The luminescent signals were detected and used for calculation of the relative cell viability (%) expressed as a percentage relative to unencapsulated cells. The cell viability of Jurkat T cells after encapsulation was also measured immediately.

Cell proliferation

Different encapsulated cells were seeded into a 96-well plate (at a concentration of 1×10^4 cells per well). Cells were incubated in a cell incubator for 24, 48, and 72 h, respectively. Following the incubation, a CellTiter 96 AQueous one solution cell proliferation assay (Promega, Madison, USA) (20 μL) was used to detect cell proliferation. This process was performed following the manufacturer instructions. Unencapsulated cells were also prepared as a control.

Enzyme-linked immunosorbent assay (ELISA)

The release of proinflammatory cytokines (IL-6, IL-2, IL-1β, and TNF-α) was measured using an ELISA kit (Biolegend, San Diego, USA). Different encapsulated cells were seeded into a 96-well plate (1×10^5 cells per well). Cells were incubated for 5 and 24 h in a cell incubator. After incubation, the supernatant of cells was collected to analyze proinflammatory cytokines.

Co-culture system

A co-culture of THP-1 macrophages and encapsulated Jurkat T cells was prepared. The macrophages at a concentration of 5×10^4 cells per well were added into a 96-well plate and were cultured for 24 h in a 5% CO_2 incubator. After culturing of THP-1 macrophages, the encapsulated Jurkat T cells at a concentration of 5×10^4 cells per well were added into a 96-well plate containing cultured macrophage cells. The cells were co-cultured for 24 h. After co-culturing for 24 h, the supernatants were collected to analyze proinflammatory cytokines.

Statistical analysis

The statistical analysis was performed by using GraphPad Prism software Version 5.0 (GraphPd Inc.). ANOVA and

Tukey–Kramer tests were used for statistical significant analysis at $P \leq 0.01$.

Results and discussion

Confirmation of cell encapsulation

To prove the encapsulation of Jurkat T cells in PAH, PSS/PAH, or PSS-GNR/PAH, numerous techniques were utilized.

First, the zeta potentials of different encapsulated Jurkat T cells were measured. Measured cells were dispersed in FBS-free RPMI-1640 for all measurements. The zeta potential value of unencapsulated Jurkat T cells was -14.3 ± 0.2 mV. However, when cells were encapsulated with PAH (PAH@Jurkat cells), the zeta potential value changed to -9.7 ± 0.2 mV. The low negative number of zeta potential value confirms that the cationic polyelectrolyte (PAH) could form a layer on the surface of the Jurkat T cells. When PAH@Jurkat cells were encapsulated with PSS-GNRs (zeta potential $\sim -16.6 \pm 0.7$ mV), the zeta potential of PSS-GNR/PAH@Jurkat cells dropped to have a lower negative value at -11.3 ± 0.4 mV. The change in zeta potential value clearly indicates that Jurkat T cells were encapsulated in PAH or PSS-GNR/PAH. Our results were similar to previous works that investigated the zeta potential values of mammalian cells coated with different polymers (Zhao et al. 2016; Pandey et al. 2013; Bondar et al. 2012). As can be seen, PAH@Jurkat cells had a weak negative value of zeta potential (-9.7 ± 0.2 mV) and the zeta potential value altered to have a further negative value after encapsulating Jurkat T cells with PSS-GNRs. The mechanism underlying the interaction in this case is unclear. We shall not discuss this in further detail, but rather mention that the charge densities of polyelectrolytes and the concentration of the ions could play a major role here. And, available results of this study strongly suggest that PSS-GNRs could modify the surface of PAH@Jurkat cells resulting in changing of zeta potential values. The binding of a weak negative charge on the cell surface to negatively charged polymers was also reported (Zhao et al. 2016). In the case of PSS/PAH@Jurkat cells, the zeta potential was more negative (-21.1 ± 0.4) than that of PSS-GNR/PAH@Jurkat cells (-11.3 ± 0.4). This could be caused by the amount of PSS formed on PSS-GNRs used in cell encapsulation, which should be less than that formed after using PSS alone. As expected, Jurkat T cells directly encapsulated in PSS had a similar zeta potential value (-14.6 ± 0.2) to unencapsulated cells (-14.3 ± 0.2). This implies that PSS could not bind well to Jurkat T cells through the same negative charge interaction of PSS and the cell membrane.

The presence of fluorescent dyes attached on PAH was used to confirm the cell encapsulation. There was no fluorescence signal detected in unencapsulated Jurkat T cells stained with FITC alone (Fig. 1a). However, FITC-positive cells were found in PAH-FITC@Jurkat cells (Fig. 1b). This indicates that cells were encapsulated with PAH. PSS/PAH@Jurkat cells stained with PAH–TRITC showed the red fluorescent signal (Fig. 1c). This confirms that PAH–TRITC could stain the cells through the PSS outer layer shielding on the Jurkat T cells. A similar result was also found in PSS-GNR/PAH@Jurkat cells (Fig. 1d). The negative control was prepared by staining PAH@Jurkat cells with PAH–TRITC. There was no presence of a red fluorescent signal. This result indicates that the same polyelectrolytes could prevent the binding between PAH and PAH-TRTIC on the cell surfaces (Fig. 1e).

We also observed the morphology of Jurkat T cells by SEM. When compared to unencapsulated cells, the appearance of a smooth surface was detected on

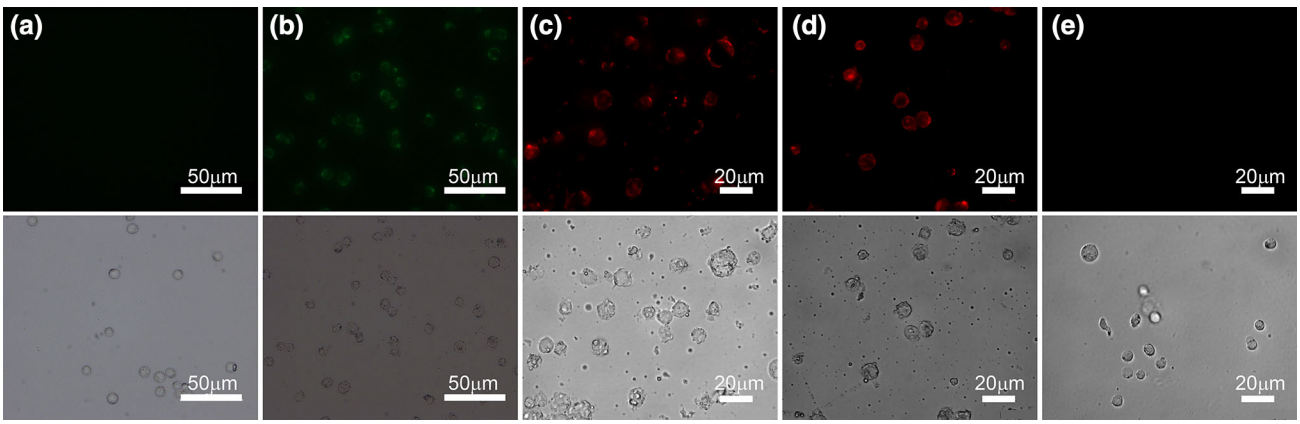

Fig. 1 Images of unencapsulated Jurkat T cells stained with FITC alone (**a**), PAH-FITC@Jurkat cells (**b**), PSS/PAH@Jurkat cells stained with PAH–TRITC (**c**), PSS-GNR/PAH@Jurkat cells stained with PAH–TRITC (**d**), and PAH@Jurkat cells with PAH–TRITC (**e**). The images were captured under bright field and fluorescent modes of a fluorescent microscope

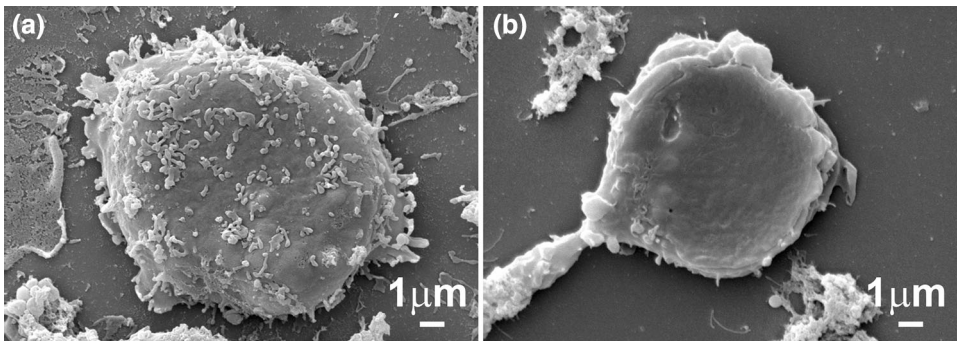

Fig. 2 SEM images of unencapsulated (**a**) and encapsulated (PSS-GNR/PAH@Jurkat) Jurkat T cell (**b**)

encapsulated cells (PSS-GNR/PAH@Jurkat cells) (Fig. 2b). However, the surfaces of unencapsulated cells had abundant microvilli (Fig. 2a). Our results are consistent with the previous work published by Zhao et al. (2016) that used chitosan and alginate to conduct a conformal encapsulation of T cells.

All approaches used for confirming the encapsulation of Jurkat T cells showed that the cells were successfully encapsulated through a layer-by-layer technique. The cationic PAH was shielded on the negative charge of the Jurkat T cell membrane. The second layer of PSS or PSS-GNRs was formed surrounding each cell. Overall results from zeta potential measurement, fluorescent observation, and SEM demonstrated the formation of different encapsulated Jurkat T cells (PAH@Jurkat, PSS/PAH@Jurkat, and PSS-GNR/PAH@Jurkat cells).

Investigation of GNRs in PAH/PSS-GNR@Jurkat cells

The ICP-MS approach was used to confirm whether PAH@Jurkat cells could be shielded by PSS-GNRs. The TEM image of PSS-GNRs is shown in Fig. 3. The data from ICP-MS showed a significant presence of gold (64.3 ± 7.7 μg L^{-1}) found in PSS-GNR/PAH@Jurkat cells (Fig. 3). The amount of gold observed provides evidence that PSS-GNRs (negatively charged surface) were shielded on the surface of PAH@Jurkat cells (positively charged cell surface) through the opposite charges of their surfaces. This result strongly indicates that a PSS-GNR layer formed on Jurkat T cells. The very small content of gold detected in PSS-GNR@Jurkat cells (1.8 ± 0.1 μg L^{-1}) could occur due to non-specific binding of PSS-GNRs to cells.

Since the ICP-MS cannot perceive the difference between GNRs deposited on the cell surface and internalized GNRs, TEM was used to evaluate how GNRs were positioned on encapsulated Jurkat T cells. With TEM images, we found that PSS-GNRs were only located on the cell surface of Jurkat T cells encapsulated PAH layers (Fig. 4c, red arrow). This strongly indicates that PSS-

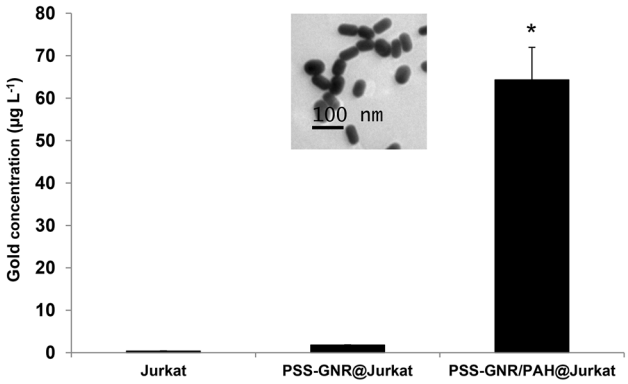

Fig. 3 The amount of gold detected in Jurkat T cells using the ICP-MS technique. *Significant difference in gold concentration at $P < 0.01$ compared with unencapsulated Jurkat T cells (Jurkat). Statistical analysis was performed by Tukey–Kramer test ($n \geq 3$). The TEM image shows the morphology of PSS-GNRs

GNRs only attached to the layer of PAH and did not internalize inside Jurkat T cells (Fig. 4c). It was reported by Fakhrullin et al. that the polyelectrolyte layer can act as a glue to attach metal nanoparticles and block nanoparticle translocation into the cells (Fakhrullin et al. 2012). As expected, there were no PSS-GNRs located on the cell surface, nor inside Jurkat T cells encapsulated with PSS/PAH (PSS/PAH@Jurkat cells; Fig. 4b) and unencapsulated Jurkat T cells (Fig. 4a). An excellent review article by Dykman and Khlebtsov (2014) has shown the effect of gold nanoparticles and their interaction with mammalian cells through cellular endocytosis. Our results here provide evidence that the PAH layer encapsulating on the cell surface might block the cellular uptake of PSS-GNRs through this endocytic pathway.

Cell viability and cell proliferation of unencapsulated and encapsulated Jurtkat cells

To investigate whether the encapsulating layers affect the cell viability, we measured the cell viability at 0 and 24 h after cultivation of unencapsulated Jurkat T cells, PAH@Jurkat cells, PSS/PAH@Jurkat cells, and PSS-GNR/

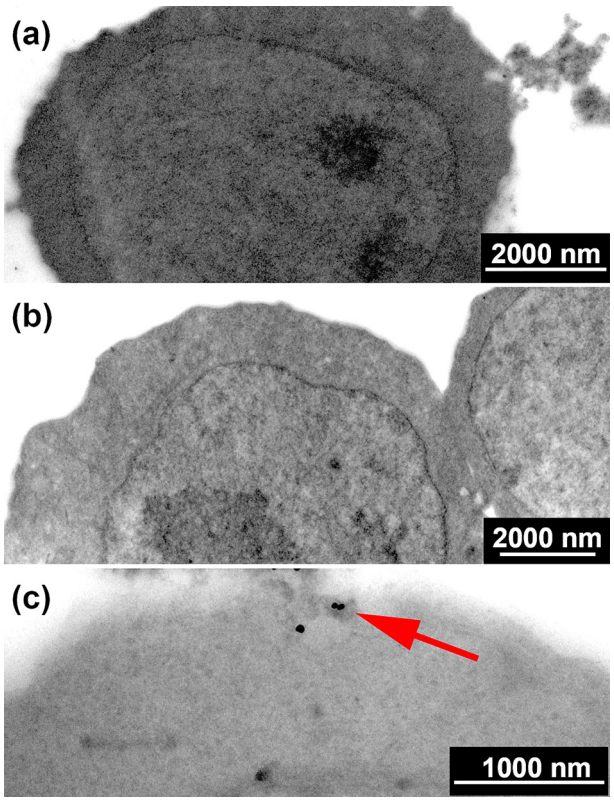

Fig. 4 TEM images of unencapsulated Jurkat T cells (**a**), PSS/PAH@Jurkat (**b**), and PSS-GNR/PAH@Jurkat cells (**c**). PSS-GNRs are located (arrow) at the cell membrane of PSS-GNR/PAH@Jurkat cells

PAH@Jurkat cells, using the CellTiter-Glo assay. This technique measured viable cells from the content of adenosine-5′-triphosphate (ATP). After encapsulation, the cell viability of PAH@Jurkat cells, PSS/PAH@Jurkat cells, and PSS-GNR/PAH@Jurkat cells was measured immediately (0 h). The relative cell viabilities, based on that of unencapsulated cells of PAH@Jurkat cells, PSS/PAH@-Jurkat cells, and PSS-GNR/PAH@Jurkat cells, were $\sim$ 94.4 $\pm$ 0.3%, 90.8 $\pm$ 1.2%, and 96.7 $\pm$ 0.9%, respectively (Fig. 5a). Significant reductions ($P < 0.01$) in cell viability were observed in encapsulated PAH@Jurkat and PSS/PAH@Jurkat cells when compared with unencapsulated cells. The lowest cell viability was detected in PSS/PAH@Jurkat cells. The cell viability after 24-h cultivation of Jurkat T cells encapsulated with different forms was also measured. It showed that the cell viability of all encapsulated cells significantly decreased ($P < 0.01$) to around 8–15% depending on the encapsulation method.

Similar to the cell viability at 0 h, PSS/PAH@Jurkat cells at 24 h showed the lowest percentage of cell viability at 85.3 $\pm$ 0.7% (Fig. 5b). The cell viabilities of PSS-GNR/PAH@Jurkat and PAH@Jurkat were 87.0 $\pm$ 0.5% and 91.5 $\pm$ 0.6%, respectively (Fig. 5b). Although the results indicate that the metabolic activity of encapsulated cells was still active after culturing for 24 h, it seems that the number of layers could influence cell viability. Cells encapsulated with a layer of PAH (PAH@Jurkat cells) had a higher cell viability than cells encapsulated with two layers (PSS/PAH@Jurkat and PSS-GNR/PAH@Jurkat cells) after 24-h cultivation. The reason for this could be that there was a higher limitation of nutrient and waste diffusion through cells in cells encapsulated with two layers than that of encapsulation with one layer.

As reported in the review paper (Antipov and Sukhorukov 2004), a higher layer number could lead to a lower amount of penetrated molecules. When compared to the cell viability between PSS/PAH@Jurkat and PSS-GNR/PAH@Jurkat cells, there was no significant difference in cell viability ($P \leq 0.01$). Furthermore, cell proliferation was determined gain more information on the metabolic function of cells after encapsulation. Unlike cell viability assay that is normally used to determine the ratio of live and dead cells, it is well known that cell proliferation assay can be used to monitor the growth rate and metabolic activity of cells.

CellTiter 96® AQueous One Solution cell proliferation assay was used to measure cell proliferation by measuring metabolic activity of cells through the reduction of MTS tetrazolium (3-(4,5-dimethylthiazol-2-yl)-5-(3-carboxymethoxyphenyl)-2-(4-sulfophenyl)-2H-tetrazolium compounds. We found that cell proliferation of PAH@-Jurkat, PSS/PAH@Jurkat, PSS-GNR/PAH@Jurkat, and Jurkat T cells was increased when we increased the culturing time from 24 h to 48 and 72 h, respectively (Fig. 6). This indicates that the encapsulation of cells, using our approach here, could influence the growth rate of Jurkat cells. However, cell proliferation of unencapsulated Jurkat T cells was much higher than that of encapsulated cells.

The relative growth rates of unencapsulated Jurkat T cells at 48 and 72 h were increased $\sim$1.4- and 2.3-fold, respectively, above unencapsulated Jurkat T cells cultured for 24 h. Around a 1.3-fold increase in the proliferation rate of PSS/PAH@Jurkat and PSS-GNR/PAH@Jurkat cells cultured for 48 h was detected as compared to encapsulated Jurkat cells after 24 h culture. The proliferation rate of PAH@Jurkat at 48 h was $\sim$ 1.1-fold increased as compared to at 24 h culture. At 72-h culture, the increase in proliferation rate of all encapsulated Jurkat T cells ($\sim$ 1.4–1.6-fold) was lower than that of unencapsulated Jurkat T cells ($\sim$ 2.3-fold) when compared to 24-h culture of each cell condition (Fig. 6). The relative proliferating cell percentages of PAH@Jurkat, PSS/PAH@Jurkat, and PSS-GNR/PAH@Jurkat cells at 24 h significantly decreased from 100% (of unencapsulated Jurkat T cells) to $\sim$ 71.9 $\pm$ 1.7%, 56.8 $\pm$ 1.1%, and 50.2 $\pm$ 1.5%,

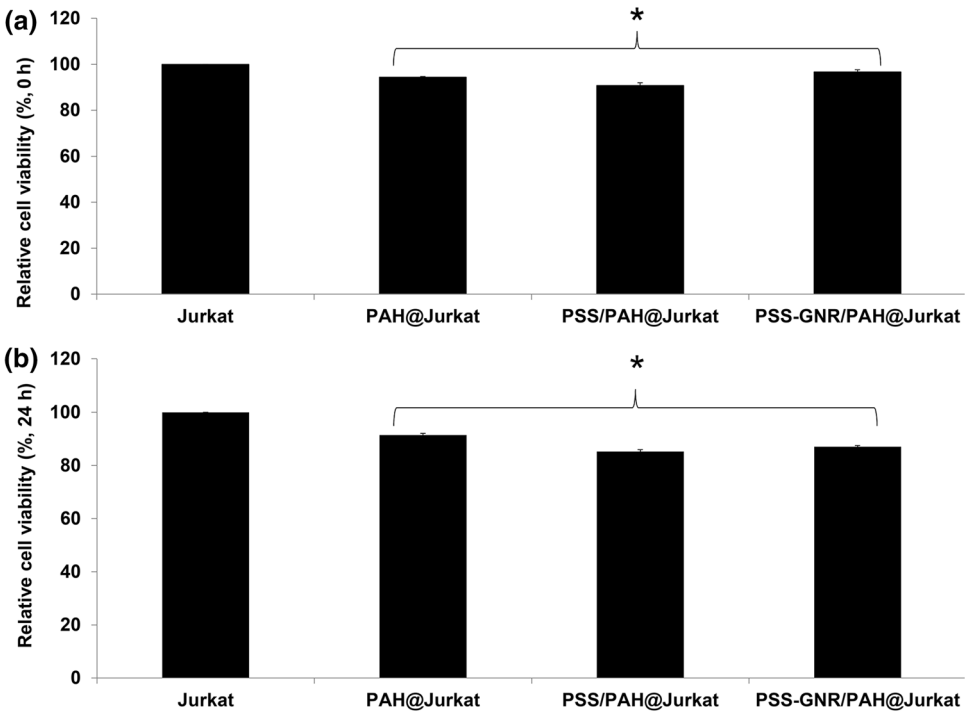

Fig. 5 Cell viability of different encapsulated Jurkat T cells at 0 h (**a**) and 24 h (**b**) compared with unencapsulated Jurkat T cells. *Significant difference in cell viability at $P < 0.01$ compared with unencapsulated Jurkat T cells (Jurkat). Statistical analysis was performed by Tukey–Kramer test ($n \geq 9$)

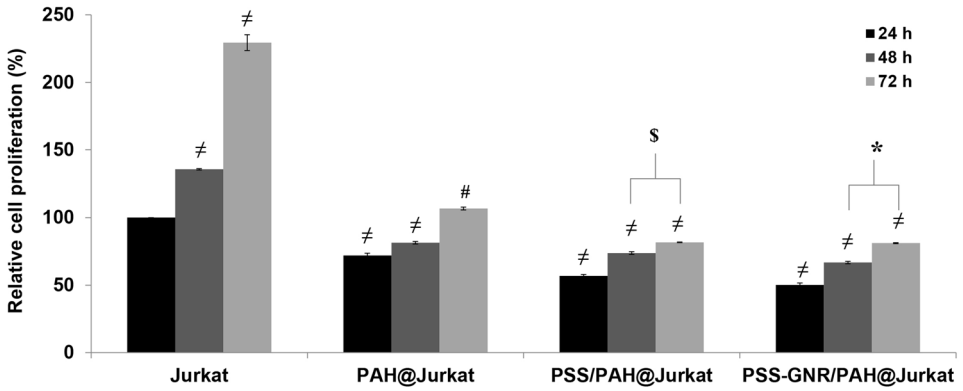

Fig. 6 Cell proliferation of unencapsulated Jurkat T cells and encapsulated Jurkat T cells at 24, 48, and 72 h. The percentage of cell proliferation is a mean value of cell proliferation relative to the control (unencapsulated Jurkat T cells cultured for 24 h). $^{\neq}$Significant difference in cell proliferation at $P < 0.01$ compared with unencapsulated Jurkat T cells (Jurkat) at 24 h. $^{\#}$Significant difference in cell proliferation at $P < 0.01$ compared with encapsulated PAH@Jurkat cells at 24 h. $^{\$}$Significant difference in cell proliferation at $P < 0.01$ compared with encapsulated PSS/PAH@Jurkat cells at 24 h. *Significant difference in cell proliferation at $P < 0.01$ compared with encapsulated PSS-GNR/PAH@Jurkat cells at 24 h. Statistical analysis was performed by Tukey–Kramer test ($n \geq 6$)

respectively. A significant decrease in proliferation rate of PAH@Jurkat, PSS/PAH@Jurkat, and PSS-GNR/PAH@Jurkat cells cultured for 48 and 72 h was also detected as compared to unencapsulated Jurkat T cells ($P < 0.01$).

At 72 h, PSS-GNR/PAH@Jurkat cells had the highest increase in growth rate ratio (~ 1.6-fold increase) among all types of encapsulated Jurkat T cells compared to a 24-h culture of encapsulated cells (PSS-GNR/PAH@Jurkat) (Fig. 6). The reason that encapsulated cells could proliferate could be a result of the mild layer-by-layer processing technique. In our case, it appears that the charge density of PAH, PSS, and PSS-GNRs might have no major effect on cell proliferation. This might be due to the low concentration of PAH, PSS, and PSS-GNRs used for cell encapsulation. Although encapsulated cells could proliferate, it seems that the encapsulating layer could reduce the rate of proliferation when compared to unencapsulated Jurkat T cells. This could have occurred due to the effect of the encapsulating layer that is possibly impacting on the diffusion rate of molecules that pass through encapsulated cells (Cook et al. 2013).

Inflammatory cytokine responses of unencapsulated and encapsulated Jurkat T cells

T cells can produce inflammatory mediators such as IL-6 and TNF-α (Wang et al. 2006). However, high secretions of IL-6 and TNF-α (Wang et al. 2006) can lead to several diseases such as cystic fibrosis (Stecenko et al. 2001), autoimmune disease, and chronic inflammatory proliferative disease (Ishihara and Hirano 2002). Hence, we investigated the secretion of these cytokines from encapsulated and unencapsulated Jurkat cells. IL-2 is a lymphokine that plays an important role in maintaining activated T cell proliferation (Pawelec et al. 1982). Therefore, we evaluated whether different encapsulations applied in our study affected the secretion of IL-2 by Jurkat T cells. Besides IL-6, TNF-α, and IL-2, we also investigated the secretion of IL-1β, another cytokine involved in inflammation induction (Tang et al. 2012).

The production of cytokines and lymphokines by encapsulated and unencapsulated Jurkat T cells was investigated at 5 and 24 h after cell encapsulation. Unencapsulated Jurkat cells were used as a control sample in our study (Fig. 7). When compared to unencapsulated Jurkat T cells, the levels of TNF-α and IL-1β at 5 h secreted by PAH@Jurkat, PSS/PAH@Jurkat, and PSS-GNR/PAH@-Jurkat cells were similar to unencapsulated Jurkat T cells (Fig. 7a, c). This indicates that the single layer (PAH) or the double layer (PSS/PAH and PSS-GNR/PAH) used for encapsulation of Jurkat T cells had no effect on TNF-α and IL-1β induction. Similar results were also observed in TNF-α production at 24 h. However, in the case of IL-1β, a significant IL-1β reduction was found in PAH@Jurkat cells after treating for 24 h ($P < 0.01$). The reason for this is uncertain. However, it is a possibility that some IL-1β molecules might not be able to pass through the PAH layer. The zeta potential of PAH@Jurkat cells was less negative than other encapsulating formats, and this could lead to different binding of PAH at the outer layer of cells to other molecules in cell culture media. This binding possibly affected IL-1β release by blocking the diffusion of IL-1β. A decrease in IL-2 levels was found in all encapsulated cells after culturing for 5 h. A significant reduction in IL-2 was detected in all encapsulated cells after cells were encapsulated and cultured for 24 h ($P < 0.01$). Werner et al. (2015) also found a reduction in IL-2 by Jurkat T cells encapsulated with polyelectrolytes (Fig. 7d).

In the case of IL-6 (Fig. 7b), at 24 h post-encapsulation, we found that cells encapsulated with PAH, PSS/PAH, and PSS-GNR/PAH secreted IL-6 at a significantly higher level than unencapsulated cells ($P < 0.01$). It was reported that the IL-6 secretion in encapsulated cells could be enhanced by polyelectrolytes used for encapsulation (Mooranian et al. 2016). Based on our results here, an induction in IL-6 levels was significantly detected in PAH@Jurkat cells at 5 h post-encapsulation. This implies that the PAH layer could first impact IL-6 induction. After cells were encapsulated with the second layer, higher levels of IL-6 were detected. Thus, the second layer of PSS or PSS-GNRs could also be involved in triggering an immune response related to IL-6 expression. Furthermore, the second layer of encapsulation might lead to a decrease in porosity that could cause an accumulation of metabolic by-products related to IL-6 production (Mooranian et al. 2016; Schmidt et al. 2008).

Biological activity in co-culture between macrophage cells and Jurkat T cells encapsulated with polyelectrolytes and PSS-coated GNRs

It is well known that macrophage cells play an important role in the immune system. Because of the lack of information on biological activities between encapsulated cells and macrophages, we were therefore interested in the biological activities of these two cells in co-culture. The co-culture system of macrophages and T cells can be used to acquire more information on immune responses between encapsulated T cells and macrophages.

We used non-activated Jurkat T cells, with and without encapsulation, to investigate whether the encapsulation of cells could influence inflammatory cytokine enhancement in the co-culture system between human macrophages and human T cells. Here, we only focused on the investigation of the double layer encapsulation (PSS/PAH@Jurkat & PSS-GNR/PAH@Jurkat cells) because we aim to use PSS-GNR/PAH@Jurkat cells in a future study for therapeutic applications. The ratio of THP-1 macrophage per Jurkat T cell used in the co-culture system was 1:1. The results showed that there were no significant differences in IL-2 and IL-1β expression in THP-1 macrophage and Jurkat T cell co-cultures when both encapsulated and unencapsulated Jurkat T cells were used (Fig. 8c, d). This implies that there was no cell-contact-mediated activation of THP-1 macrophages by encapsulated and unencapsulated Jurkat T cells. As stated previously, TNF-α and IL-6 cytokines are inflammatory cytokines and they may be involved in some disease pathogenesis (Rossol et al. 2005). Therefore, it was also worthwhile to test whether encapsulated cells could lead to induction of IL-6 and TNF-α expression.

Our results showed that there was a significant induction of TNF-α in THP-1 macrophages/unencapsulated Jurkat T cells after co-culturing for 24 h when compared with THP-1 macrophages cultured alone. However, there was no increase in TNF-α level when THP-1 macrophages were cultured with encapsulated Jurkat T cells (PSS/PAH@Jurkat or PSS-GNR/PAH@Jurkat) (Fig. 8b). These results

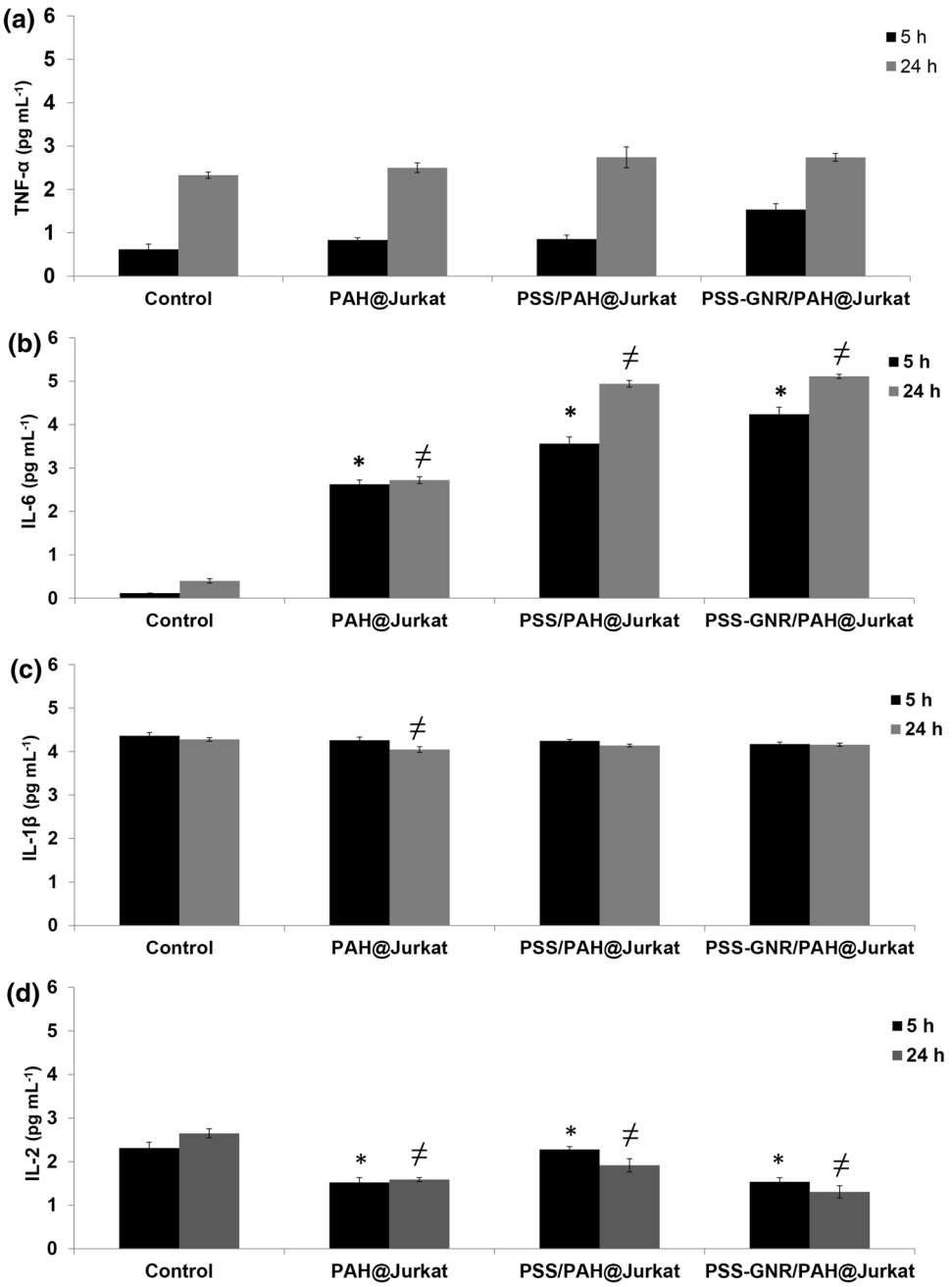

Fig. 7 Different pro-inflammatory responses of TNF-α (**a**), IL-6 (**b**), IL-1β (**c**), and IL-2 (**d**) from each type of encapsulated and unencapsulated cells at 5 and 24 h post-encapsulation. *Significant difference in pro-inflammatory responses at $P < 0.01$ compared with unencapsulated cells at 5 h and ≠ at 24 h. Statistical analysis was performed by Tukey–Kramer test ($n \geq 4$)

indicate that the encapsulation of Jurkat T cells could help prevent the induction of TNF-α production through cell-contact-mediated activation of THP-1 macrophages by Jurkat T cells. The layer of PSS/PAH or PSS-GNR/PAH could block the ligand interactions involved in TNF-α production by THP-1 macrophages resulting in no activation of the THP-1 macrophages to enhance TNF-α production. The TNF-α levels in co-cultures of THP-1 macrophages with PSS/PAH@Jurkat or PSS-GNR/PAH@Jurkat cells were similar. This implies that GNRs had no impact on inducing TNF-α. These two types of cell encapsulation resulted in different zeta potential values (-21.1 ± 0.4 for PSS/PAH@Jurkat and -11.3 ± 0.4 for PSS-GNR/PAH@Jurkat cells), but it seems that the different degree of zeta potential values did not impact on the induction of TNF-α in our system.

In the case of IL-6 expression, we found that there was no significant difference in IL-6 production of THP-1 macrophage/Jurkat T cell (both unencapsulated and encapsulated cells) co-cultures. These results also revealed that there was no cell-contact-mediated activation of THP-1 macrophages through ligand interactions by encapsulated and unencapsulated Jurkat T cells (Fig. 8a). However, it is worth noting that though, there was an induction of IL-6 in

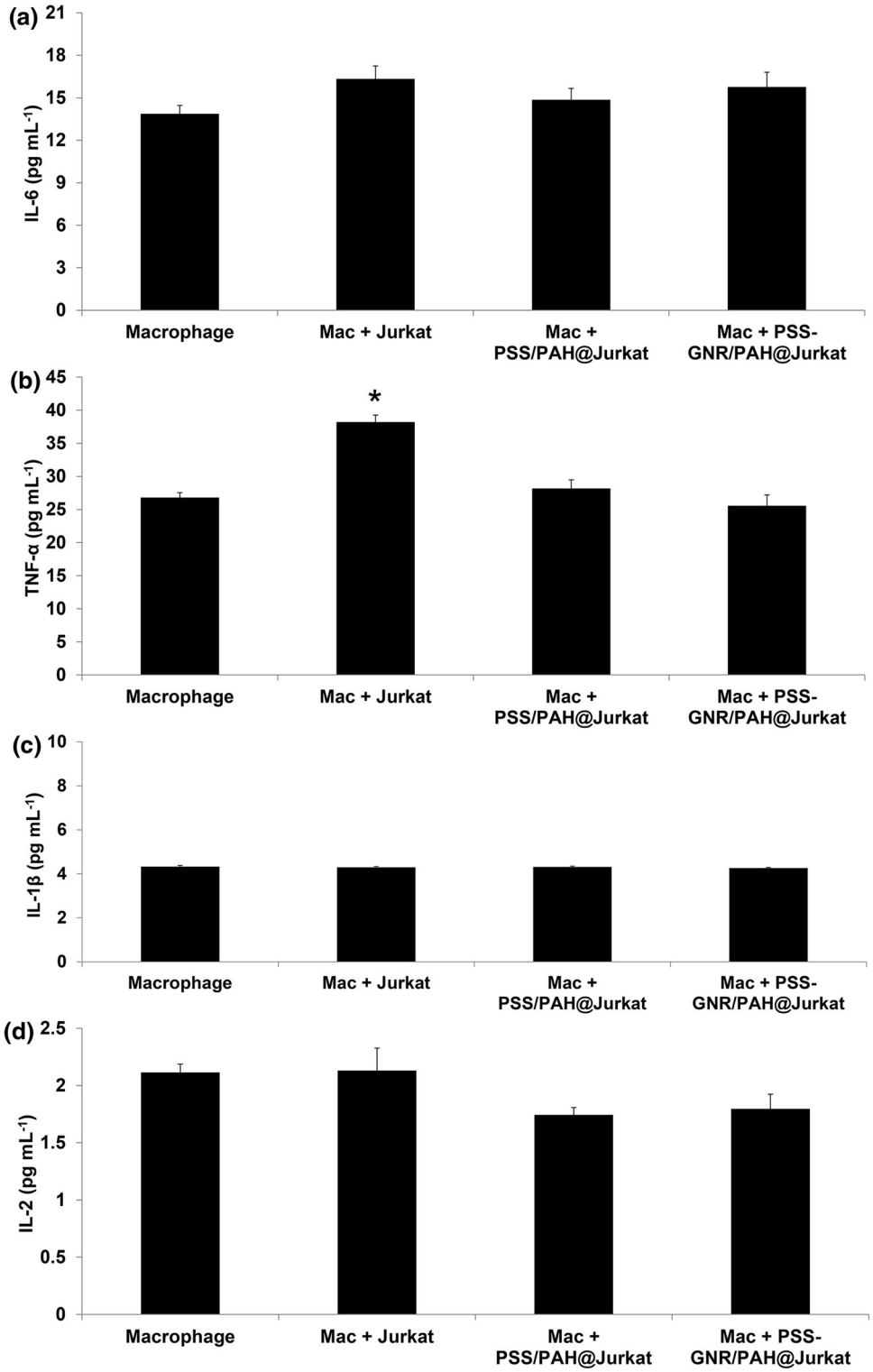

Fig. 8 The expression of inflammatory cytokines IL-6 (**a**), TNF-α (**b**), IL-1β (**c**), and IL-2 (**d**) in THP-1 macrophages co-cultured with unencapsulated and encapsulated Jurkat T cells. Two different types of encapsulated Jurkat T cells (PSS/PAH@Jurkat and PSS-GNR/PAH@Jurkat) were used in this co-culture system. *Significant difference in TNF-α level at $P < 0.01$ compared with THP-1 macrophages alone. Statistical analysis was performed by Tukey–Kramer test ($n \geq 7$)

encapsulated Jurkat T cells. Nonetheless, the induction amount of IL-6 was much lower than Jurkat cells treated with a positive control chemical (phorbol 12-myristate 13-acetate; PMA) (Supplementary Material, Fig. S1) and there was no significant production of IL-6 in THP-1 macrophage/Jurkat T cell co-culture. This implies that the induction amount of IL-6 in encapsulated Jurkat T cells might be at a level that does not lead to an adverse effect.

Conclusions

We demonstrate a single-cell encapsulation of Jurkat T cells and biological activities of cells after encapsulation. Jurkat T cells were successfully encapsulated with PAH, PSS/PAH, or PSS-GNR/PAH. Encapsulated cells mostly maintained viability and their metabolic activity. This could be due to the mild interaction between PAH, PSS/PAH, or PSS-GNR/PAH and the cell membrane. The cell proliferation assay confirmed that encapsulated cells were capable of cell division, and PSS-GNR/PAH@Jurkat cells had the highest cell proliferation rate. In THP-1 macrophage/Jurkat cell co-cultures, the encapsulation of Jurkat T cells could shield some cell surface functions that impacts cell-to-cell signaling between THP-1 macrophages and Jurkat T cells, resulting in no induction of TNF-α or other cytokines observed in the co-cultures. Unlike the macro- or microcapsule cell encapsulation technique, cells were singly encapsulated with a thin layer of polyelectrolytes and polyelectrolyte-coated GNRs, which had no significant effect on cell size. Therefore, this technique should avoid the problem of blood flow blockage when cells are applied in a blood circulation system. As well, with the property of GNRs mentioned earlier, to combine GNRs on a layer of encapsulated cells should help increase the efficiency for diagnostic or therapeutic purposes. Overall, the assessment of biological activities found in this study suggests that the combination of polyelectrolytes and GNRs for single-cell encapsulation was reasonably biocompatible with Jurkat T cells and macrophages. The results from this study support continuing and further developing studies based on using this encapsulation technique, combined with GNRs, in various biomedical applications without adverse inflammatory effects.

Acknowledgements This work was fully supported by the Thailand Research Fund (TRF; RSA5880011), Mahidol University, and Faculty of Science, Mahidol University. The authors thank the Center of Nanoimaging and Center of Excellent on Environmental Health and Toxicology, Faculty of Science, Mahidol University for providing some facilities used for this research. We also thank Dr. Sujin Jiracheewanun and Mr. Pongsak Prasertphol for their technical supports.

References

Ai H, Jones SA, Lvov YM (2003) Biomedical applications of electrostatic layer-by-layer nano-assembly of polymers, enzymes, and nanoparticles. Cell Biochem Biophys 39:23

Antipov AA, Sukhorukov GB (2004) Polyelectrolyte multilayer capsules as vehicles with tunable permeability. Adv Colloid Interface Sci 111:49–61

Bhatia SR, Khattak SF, Roberts SC, Uludag H (2005) Polyelectrolytes for cell encapsulation. Curr Opin Colloid Interface Sci 10:45–51

Bondar OV, Saifullina DV, Shakhmaeva II, Mavlyutova II, Abdullin TI (2012) Monitoring of the zeta potential of human cells upon reduction in their viability and interaction with polymers. Acta Naturae 4:78–81

Borkowska M, Grzeczkowicz A, Strawski M, Kawiak J, Szklarczyk M, Granicka LH (2014) Performance and detection of nano-thin polyelectrolyte shell for cell coating. J Nanopart Res 16:2488

Bray D (2000) Critical point drying of biological specimens for scanning electron microscopy. Supercrit Fluid Methods Protoc 13:235–243

Cook MT, Tzortzis G, Khutoryanskiy VV, Charalampopoulos D (2013) Layer-by-layer coating of alginate matrices with chitosan-alginate for the improved survival and targeted delivery of probiotic bacteria after oral administration. J Mater Chem B 1:52–60

de Vos P, Lazarjani HA, Poncelet D, Faas MM (2014) Polymers in cell encapsulation from an enveloped cell perspective. Adv Drug Deliv Rev 67–68:15–34

Diaspro A, Silvano D, Krol S, Cavalleri O, Gliozzi A (2002) Single living cell encapsulation in nano-organized polyelectrolyte shells. Langmuir 18:5047–5050

Dykman LA, Khlebtsov NG (2014) Uptake of engineered gold nanoparticles into mammalian Cells. Chem Rev 14:1258–1288

Fakhrullin RF, Zamaleeva AI, Morozov MV, Tazetdinova DI, Alimova FK, Hilmutdinov AK, Zhdanov RI, Kahraman M, Culha M (2009) Living fungi cells encapsulated in polyelectrolyte shells doped with metal nanoparticles. Langmuir 25:4628–4634

Fakhrullin RF, Zamaleeva AI, Minullina RT, Konnova SA, Paunov VN (2012) Cyborg cells: functionalisation of living cells with polymers and nanomaterials. Chem Soc Rev 41:4189–4206

Franz B, Balkundi SS, Dahl C, Lvov YM, Prange A (2010) Layer-by-layer nano-encapsulation of microbes: controlled cell surface modification and investigation of substrate uptake in bacteria. Macromol Biosci 10:164–172

Granicka LH, Borkowska M, Grzeczkowicz A, Stachowiak R, Szklarczyk M, Bielecki J, Strawski M (2014) The targeting nanothin polyelectrolyte shells in system with immobilized bacterial cells for antitumor factor production. J. Biomed. Mater. Res. A 102:2662–2668

Gurruchaga H, Saenz del Burgo L, Ciriza J, Orive G, Hernández RM, Pedraz JL (2015) Advances in cell encapsulation technology and its application in drug delivery. Expert Opin. Drug Deliv. 12:1251–1267

Hachim D, Melendez J, Ebensperger R (2013) Nanoencapsulation of Human Adipose Mesenchymal Stem Cells: experimental Factors Role to Successfully Preserve Viability and Functionality of Cells. J. Encapsulation Adsorpt. Sci. 3:1–12

Heckman C, Kanagasundaram S, Cayer M, Paige J (2007) Preparation of cultured cells for scanning electron microscope. Nat Protoc. doi:10.1038/nprot.2007.504

Hunt NC, Grover LM (2010) Cell encapsulation using biopolymer gels for regenerative medicine. Biotechnol Lett 32:733–742

Ishihara K, Hirano T (2002) IL-6 in autoimmune disease and chronic inflammatory proliferative disease. Cytokine Growth Factor Rev 13:357–368

Juan FV, Malcolm KB, Gianpietro D (2009) Immunotherapy of human cancers using gene modified T lymphocytes. Curr Gene Ther 9:396–408

Kampf N (2002) The use of polymer for coating cells. Polym Adv Technol 13:896–905

Kim C, Agasti SS, Zhu Z, Isaacs L, Rotello VM (2010) Recognition-mediated activation of therapeutic gold nanoparticles inside living cells. Nat Chem 2:962–966

Mooranian A, Negrulj R, Al-Salami H, Morahan G, Jamieson E (2016) Designing anti-diabetic β-cells microcapsules using polystyrenic sulfonate, polyallylamine, and a tertiary bile acid: morphology, bioenergetics, and cytokine analysis. Biotechnol Prog 32:501–509

Orive G, Santos E, Pedraz JL, Hernández RM (2014) Application of cell encapsulation for controlled delivery of biological therapeutics. Adv Drug Deliv Rev 67–68:3–14

Pandey S, Afrin F, Tripathi RP, Gangenahalli G (2013) Human T-cell line (Jurkat cell) encapsulation by nano-organized polyelectrolytes and their response assessment in vitro and in vivo. J Nanopart Res 15:1793

Pawelec G, Borowitz A, Krammer PH, Wernet P (1982) Constitutive interleukin 2 production by the Jurkat human leukemic T cell line. Eur J Immunol 12:387–392

Pissuwan D, Niidome T (2015) Polyelectrolyte-coated gold nanorods and their biomedical applications. Nanoscale 7:59–65

Pissuwan D, Kumagai Y, Smith NI (2013) Effect of surface-modified gold nanorods on the inflammatory cytokine response in macrophage cells. Part Part Syst Char 30:427–433

Roncarolo M-G, Battaglia M (2007) Regulatory T-cell immunotherapy for tolerance to self antigens and alloantigens in humans. Nat Rev Immunol 7:585–598

Rossol M, Kaltenhäuser S, Scholz R, Häntzschel H, Hauschildt S, Wagner U (2005) The contact-mediated response of peripheral-blood monocytes to preactivated T cells is suppressed by serum factors in rheumatoid arthritis. Arthritis Res Ther 7:R1189–R1199

Schmidt JJ, Rowley J, Kong HJ (2008) Hydrogels used for cell-based drug delivery. J Biomed Mater Res A 87A:1113–1122

Stecenko AA, King G, Torii K, Breyer RM, Dworski R, Blackwell TS, Christman JW, Brigham KL (2001) Dysregulated cytokine production in human cystic fibrosis bronchial epithelial cells. Inflammation 25:145–155

Tang A, Sharma A, Jen R, Hirschfeld AF, Chilvers MA, Lavoie PM, Turvey SE (2012) Inflammasome-mediated IL-1β production in humans with cystic fibrosis. PLoS One 7:e37689

Uludag H, De Vos P, Tresco PA (2000) Technology of mammalian cell encapsulation. Adv Drug Deliv Rev 42:29–64

Wang J, Shannon MF, Young IG (2006) A role for Ets1, synergizing with AP-1 and GATA-3 in the regulation of IL-5 transcription in mouse Th2 lymphocytes. Int Immunol 18:313–323

Werner M, Schmoldt D, Hilbrig F, Jérôme V, Raup A, Zambrano K, Hübner H, Buchholz R, Freitag R (2015) High cell density cultivation of human leukemia T cells (Jurkat cells) in semipermeable polyelectrolyte microcapsules. Eng Life Sci 15:357–367

Winky LWH, Dieter WT, Nikolaus JS, Man W, Yitshak Z (2003) Surface-chemistry technology for microfluidics. J Micromech Microeng 13:272

Zhao S, Zhang L, Han J, Chu J, Wang H, Chen X, Wang Y, Tun N, Lu L, Bai X-F, Yearsley M, Devine S, He X, Yu J (2016) Conformal nanoencapsulation of allogeneic T cells mitigates graft-versus-host disease and retains graft-versus-leukemia activity. ACS Nano 10:6189–6200

Publisher's Note

Effect of encapsulated cytotoxic T-cells on cancer cell destruction

Author: Porntida Wattanakull, Dakrong Pissuwan
Materials Science and Engineering Program, Multidisciplinary Unit,
Faculty of Science, Mahidol University

Abstract

Cytotoxic T-cells can destroy cancer cells by releasing cytotoxic molecules to attack cancer cells. Therefore, the cell therapy by implanting cytotoxic T–cells for cancer treatment has been of interest. However, to avoid the reaction of the immune system on the implanted cells, the encapsulation technique has been applied. In this study, the encapsulated cytotoxic T-cells were used for destroying breast cancer cells (MCF-7 cells). Cytotoxic T-cells were encapsulated in poly(allylamine hydrochloride) (PAH) as a first encapsulating layer and poly(styrene sulfonate) (PSS) as a second layer. Thereafter, encapsulated cytotoxic T-cells were co-cultured with MCF-7 cells. When compared with the control cells (MCF-7 cells cultured alone), the results showed the significant percentage of dead MCF-7 cells at 13.11±1.2 in MCF-7 cells co-cultured with encapsulated cytotoxic T-cells, as compared to MCF-7 cells co-cultured with non-encapsulated cytotoxic T cells, which had the percentage of dead MCF-7 at 14.67±1.2. This implies that the encapsulation of cytotoxic cells could remain some cell functions that could involve in cancer cell destruction.

Key Word (s): Cytotoxic T-cells, Cell encapsulation, Cancer cells

Introduction

It is well-known that T lymphocyte cells (T-cells) are a main player in an adaptive immune system. In the environment containing pathogens or malignancies, effector T-cells called cytotoxic T-cells could work on specific target cell (TC) destruction based on their antigen-specific receptor and their ability to release toxic molecules. Therefore, the use of cytotoxic T-cells for TC destruction has been applied in the field of immunotherapy. It was reported that T-cells could be induced to cytotoxic T cells by activating with anti-CD3 antibodies (Tsoukas et al. 1985). After activation, these cytotoxic T-cells could destroy infected cells and tumor cells (de Alborán et al. 2003, Lindsten et al. 1989, Smith-Garvin, Koretzky, and Jordan 2009, Wajant, Gerspach, and Pfizenmaier 2005). However, these cytotoxic T-cells could also affect healthy cells. Furthermore, in the case of implanted cytotoxic T-cells into the body for cancer therapy, these cells may also face with the host immune reaction of the immune system.

Recently, cell encapsulation has been proposed to avoid implanted cells from the host immune reaction (de Vos, Hamel, and Tatarkiewicz 2002, Hernández et al. 2010, Lim and Sun 1980, Lund-Johansen 2003). Cell encapsulation can be done by immobilizing living cells within the polymer matrix. The polymer used for encapsulation should act as a semi-permeable membrane that can allow the diffusion of small molecules such as oxygen and nutrients between inside and outside cells. This diffusion helps maintain the cell viability and also helps implanted cells escaping from immune cells and some antibodies (Lim et al. 2010, Orive et al. 2004, Uludag, de Vos, and Tresco 2000). Some reports have shown that encapsulated living cells

could release important molecules for some therapeutics use (Goren et al. 2010, Uludag, de Vos, and Tresco 2000). Due to this reason, we were interested to encapsulate cytotoxic T-cells with polyelectrolyte polymers and investigated the possibility of using encapsulated cytotoxic T-cells for cancer treatment. In this study, the MCF-7 cells were used as a model cancer cell.

Therefore, in this study we activated T-cells with anti-CD3 anibodies and encapsulated activated T-cell (cytotoxic T-cells) with poly(allylamine hydrochloride) (PAH) and poly(styrene sulfonate) (PSS). After encapsulation, the ability of encapsulated cytotoxic T-cells for killing cancer cells was observed by co-culturing with breast cancer cell (MCF-7 cells).

Objectives

1) To activate T-cells to cytotoxic T-cell with anti-CD3 antibodies.
2) To encapsulate cytotoxic T-cell.
3) To investigate the cancer destruction of encapsulated and non-encapsulated cytotoxic T-cells.

Research Methodology

Cell preparation. MCF-7 cells were cultured in Dulbecco's Modified Eagle's Medium (DMEM) plus Minimum Essential Medium (MEM) (DMEM: MEM = 1:1) supplemented with 10% of fetal bovine serum (FBS). The media were added with 1% penicillin and streptomycin and cells were incubated at 37^{o}C in a 5% CO_2 incubator. T-cells used in this study were separated from peripheral blood mononuclear cells (PBMCs). PBMCs were cultured in DMEM without FBS for 3 h. Then, non-adherent cells (T-cells) were collected from the culture dish. The separated T-cells were cultured in Roswell Park Memorial Institute (RPMI) 1640 medium supplemented with 10% FBS plus 1% penicillin and streptomycin. The cells were also incubated in an incubator at the same condition used for MCF-7 cells.

Cytotoxic T-cell preparation. A 96 well plate were coated with a 50 µl of anti-CD3 antibodies (clone: HIT3a; antibodies 0.05 µg/ml). The plate was incubated at 4^{o}C overnight. After incubation, the antibody solution was removed and the plate was washed 3 times with sterile phosphate buffer saline (PBS). The suspension of T-cells ($1x10^6$ cells/ml) was dispersed in culture media and a 200 µl of T-cells was added into a 96-well plate coated with anti-CD3 antibodies. Next, the culture was incubated at 37^{o}C in a 5% a CO_2 incubator for 3 days. Finally, T-cells were activated and changed to cytotoxic T-cells. This change was confirmed by cytotoxic molecule detection. These cytotoxic T-cells were stored in liquid nitrogen for using in further experiments.

Cell encapsulation. Two polyelectrolytes were used to encapsulate cells. The first layer of cytotoxic T-cells was coated with PAH, which is a cationic polymer. Cytotoxic T-cells (at the number of $1x10^6$ cells in 1 ml of cell culture medium containing FBS) were centrifuged at 6500 rpm for 5 min. The pellet after centrifugation was dispersed in a 1 ml of RPMI without FBS. A 500 µl of 0.05 mg/ml PAH was added into cell suspension and the cell suspension was mixed on a shaker for 5 min. After that, cells were centrifuged to obtain PAH-encapsulated cells and the free PAH was removed by washing with RPMI without FBS. Thereafter, cytotoxic T-cells were mixed with 0.1 mg/ml PSS (anionic polymer) on a shaker for 10 min. The

PSS formed a second encapsulating layer on the surface of cytotoxic T-cells. Similar to PAH, the free PSS was removed by washing as described previously. Finally, cytotoxic T-cells encapsulated with PAH/PSS were suspended in RPMI-1640 medium. These cells were called as "PSS/PAH@CT" cells. The normal T-cells encapsulated with PAH/PSS were also prepared using the same procedure. T-cells encapsulated with PAH/PSS were called as "PSS/PAH@lym" cells.

Cancer destruction by encapsulated cytotoxic T-cell. The MCF-7 cells at a number of $1x10^4$ cells (with a volume of 100 µl) were added into a 24-well plate. The cells were cultured for 24 h at 37°C in a 5% CO_2 incubator. After incubation, PSS/PAH@CT, PSS/PAH@lym non-encapsulated T-cells, and non-encapsulated cytotoxic T-cells at a number of $4x10^5$ cells (with a volume of 100 µl) were added into a 24-well plate containing MCF-7 cells. This was a co-culture with each form of T-cells and MCF-7 cells. The co-culture of cells was incubated for 24 h. After incubation, PSS/PAH@lym, PSS/PAH@CT, non-encapsulated T-cells, and non-encapsulated cytotoxic T-cells were removed from the plate by washing 3 times with PBS containing Ca^{2+} and Mg^{2+} to avoid the detachment of cancer cells. Then, a 150 µl of RPMI without FBS was added into a 24-well plate containing MCF-7 cells. Next, a 150 µl of trypan blue was added into a 24-well plate and incubated for 5 min. After that, the trypan blue was removed and the MCF-cells in a well plate were washed 2 times with PBS containing Ca^{2+} and Mg^{2+}. The dead MCF-7 cells stained with blue colour were observed under inverted microscope (15-20 fields per condition and each condition was run for 3 sets).

Statistical Analysis. The data were expressed as mean ± standard error (SE) which was analyzed by using one-way analysis of variance (ANOVA) following by Tukey's multiple comparison test using GraphPad Prism® Version 6. Statistical significance was considered as significance at 95% confidence.

Results

T-cells and cytotoxic T-cells could be encapsulated with PAH/PSS. After encapsulation, their relative cell viability compared to non-encapsulated cells was dropped from 100% to 73.19%±0.5 for PSS/PAH@lym cells and 71.50%±1.0 for PSS/PAH@CT cells (Figure 1).

As mentioned previously, cytotoxic T-cells can destroy cancer cells. Thus, to investigate whether encapsulated cytotoxic T-cells could destroy cancer cells, PSS/PAH@CT cells were co-cultured with MCF-7 cells for 24 h. After culturing, the dead MCF-7 cells were observed by staining with trypan blue. The results showed that the dead MCF-7 cells (shown in blue) were detected in MCF-7 cells co-cultured with non-encapsulated cytotoxic T-cells (Figure 2D) and PSS/PAH@CT cells (Figure 2E). As expected, there were no dead MCF-cells after co-culturing with normal T-cells with and without encapsulation (Figure 2B&C). These results confirmed that encapsulated cytotoxic T-cells still had an ability to destroy MCF-cells.

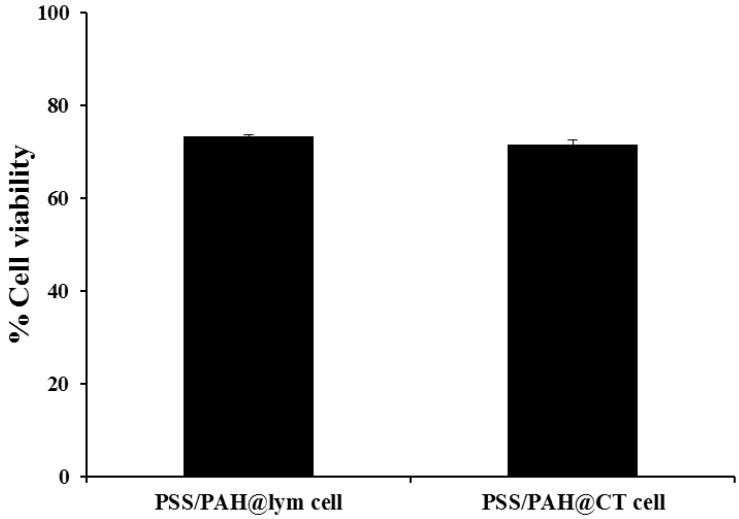

Figure 1. Cell viability of T-cells and cytotoxic T-cell encapsulated with PAH and PSS.

In the case of MCF-7 cells cultured alone, it also found that cells were healthy (Figure 2A). The percentage of dead MCF-7 cells after co-culturing with different forms of T-cells was shown in Figure 3.

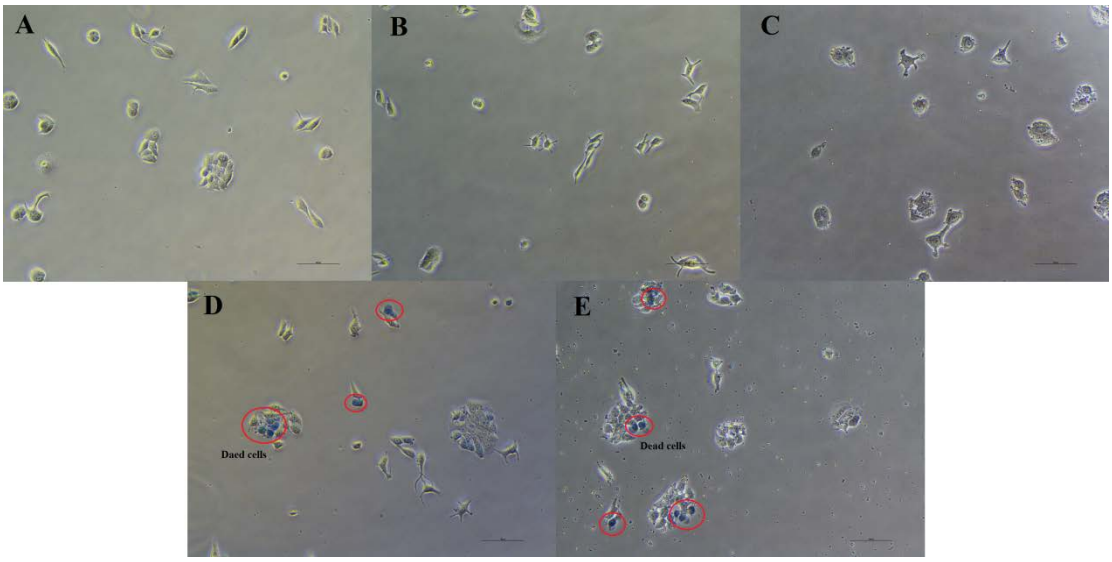

Figure 2. The bright field image of MCF-7 cells cultured alone (A) and MCF-7 cells after co-cultured with: normal T-cells (B), encapsulated normal T-cells cells (C), non-encapsulated cytotoxic T-cells (D), and encapsulated cytotoxic T-cells (E) for 24 h and stained with trypan blue.

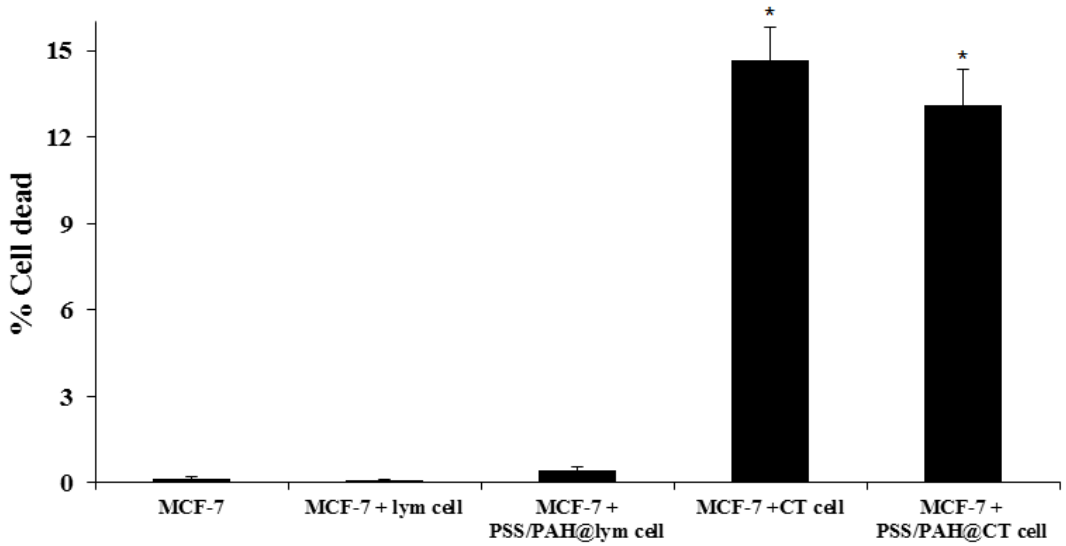

Figure 3. The percentage of dead MCF-7 cells co-cultured with T-cells (lym cells), cytotoxic T-cells (CT cells), PSS/PAH@lym cells (encapsulated T-cells), and PSS/PAH@CT cells (encapsulated cytotoxic T-cells). * Significant difference from MCF-7 cells cultured alone (control) at $p < 0.05$.

The small number of dead cells at ~ 0.16±0.1% was detected in MCF-7 cells. The numbers of dead MCF-7 cells co-cultured with normal T-cells and PSS/PAH@lym cells were similar to MCF-7 cells cultured alone. However, when MCF-7 cells were co-cultured with cytotoxic T-cells and PSS/PAH@CT cells, the percentage of dead MCF-7 cells was significantly increased to ~14.67±1.2% (for MCF-7 cells co-cultured with cytotoxic T-cells) and 13.11±1.2% (for MCF-7 cells co-cultured with PSS/PAH@CT cells) after comparing to MCF-7 cells cultured alone.

Discussion

T-cells could be stimulated to cytotoxic T-cells by using anti-CD3 antibodies. When cytotoxic T-cells were cultured with cancer cells (MCF-7 cells), the dead MCF-7 cells were detected. It was reported that cytotoxic T-cells could destroy cancer cells through three possible pathways (Andersen et al. 2006). First, cytotoxic T-cells may kill cancer cells by releasing cytokines such as tumour necrosis factor-α and IFN-γ (interferon-gamma) resulting in induction of target cell death. Second, the interaction between cytotoxic T-cells and target cells may lead to apoptotic cell death through receptor triggering. And third, the release of cytotoxic molecules (perforin and granzymes) can destroy their target cells. The results here could confirm that cytotoxic T-cells could destroy MCF-7 cancer cells. As well, encapsulated cytotoxic T-cells (PSS/PAH@CT cells) could effectively destroy MCF-7 cancer cells. However, the pathway of cancer destruction between encapsulated and non-encapsulated cytotoxic T-cells might be different. As shown in Figure 3, the percentage of cell death of MCF-7 cells co-cultured with PSS/PAH@CT cells was lower than that of MCF-7 cells co-cultured with non-encapsulated cytotoxic T-cells. This implies that PSS/PAH@CT cells might destroy MCF-7 cells through indirect pathway by releasing toxic cytokines to destroy MCF-7 cells. The direct killing of MCF-7 cells by PSS/PAH@CT cells through receptor could be hardly occurred

because the surface of cytotoxic T-cells was encapsulated with PAH and PSS. In the case of non-encapsulated cytotoxic T-cells, the destruction of MCF-7 cells might occur through all possible mechanisms mentioned above resulting in more efficiency in killing MCF-7 cells. This outcome provides useful data to further develop the use of encapsulated cytotoxic T-cells for cancer therapy.

Recommendations

The outcome of this work has shown that encapsulated cytotoxic T-cells were capable to destroy cancer cells (MCF-7 cells) that used as a model cell in this study. The further work on detections of cytokines and toxic molecules involving in cancer destruction should be further performed to clearly understand the mechanism of cancer destruction by encapsulated cytotoxic T-cells. This information can be used to further development encapsulated cytotoxic T-cells for cancer therapy.

References

Alborán, Ignacio Moreno, Marı Robles, x, S. a, Alexandra Bras, Esther Baena, Martı, x, and Carlos nez-A. (2003). "Cell death during lymphocyte development and activation." **Seminars in Immunology** 15, 3: 125-133.

Andersen, Mads Hald, David Schrama, Per thor Straten, and Jürgen C. Becker. (2006). "Cytotoxic T Cells." **Journal of Investigative Dermatology** 126, 1: 32-41.

de Alborán, Ignacio Moreno, Marı Robles, x, S. a, Alexandra Bras, Esther Baena, Martı, x, and Carlos nez-A. (2003). "Cell death during lymphocyte development and activation." **Seminars in Immunology** 15, 3: 125-133.

de Vos, P., A. F. Hamel, and K. Tatarkiewicz. (2002). "Considerations for successful transplantation of encapsulated pancreatic islets." **Diabetologia** 45, 2: 159-173.

Goren, Amit, Nitsan Dahan, Efrat Goren, Limor Baruch, and Marcelle Machluf. (2010). "Encapsulated human mesenchymal stem cells: a unique hypoimmunogenic platform for long-term cellular therapy." **The FASEB Journal** 24, 1: 22-31.

Hernández, Rosa M., Gorka Orive, Ainhoa Murua, and José Luis Pedraz. (2010). "Microcapsules and microcarriers for in situ cell delivery." **Advanced Drug Delivery Reviews** 62, 7–8: 711-730.

Lim, F, and AM Sun. (1980). "Microencapsulated islets as bioartificial endocrine pancreas." **Science** 210, 4472: 908-910.

Lim, G. J., S. Zare, M. Van Dyke, and A. Atala. (2010). "Cell microencapsulation." **Adv Exp Med Biol** 670: 126-136.

Lindsten, Tullia, Carl H. June, Jeffrey A. Ledbetter, Gregory Stella, and Craig B. Thompson. (1989). "Regulation of lymphokine messenger RNA stability by a surface-mediated T cell activation pathway." **Science** 244: 339+.

Lund-Johansen, Therese Visted and Morten. (2003). "Progress and challenges for cell encapsulation in brain tumour therapy." **Expert Opinion on Biological Therapy** 3, 4: 551-561.

Orive, Gorka, Rose Maria Hernández, Alicia Rodríguez Gascón, Riccardo Calafiore, Thomas Ming Swi Chang, Paul de Vos, Gonzalo Hortelano, David Hunkeler, Igor Lacík, and José Luis Pedraz. (2004). "History, challenges

and perspectives of cell microencapsulation." **Trends in Biotechnology** 22, 2: 87-92.

Smith-Garvin, Jennifer E., Gary A. Koretzky, and Martha S. Jordan. (2009). "T Cell Activation." **Annual review of immunology** 27: 591-619.

Tsoukas, C D, B Landgraf, J Bentin, M Valentine, M Lotz, J H Vaughan, and D A Carson. (1985). "Activation of resting T lymphocytes by anti-CD3 (T3) antibodies in the absence of monocytes." **The Journal of Immunology** 135, 3: 1719-1723.

Uludag, Hasan, Paul de Vos, and Patrick A. Tresco. (2000). "Technology of mammalian cell encapsulation." **Advanced Drug Delivery Reviews** 42, 1–2: 29-64.

Wajant, Harald, Jeannette Gerspach, and Klaus Pfizenmaier. (2005). "Tumor therapeutics by design: targeting and activation of death receptors." **Cytokine & Growth Factor Reviews** 16, 1: 55-76.